

**Software Development for Beam Cooling Simulation
Including General Collider Physics**

Final report

to the Accord

between Brookhaven National Laboratory (BNL)
and Joint Institute for Nuclear Research (JINR)

I.N.Meshkov, A.O. Sidorin, A.V.Smirnov, G.V.Trubnikov
Joint Institute for Nuclear Research, Dubna, Russia

September 2006

Abstract

This report summarizes results of the software development during the period from August 1, 2005 to August 1, 2006. The code benchmarking and support will continue during 1-year service term until August 2007.

General attention at this stage of the work was devoted to development of the electron cooling models in order to provide realistic comparison between non-magnetized cooling force calculation and experiments at Fermilab Recycler ring. Algorithm for stochastic cooling and optical stochastic cooling simulation was introduced. New algorithms for calculation of the electron cooling friction force with real distribution of electron bunch were implemented.

Contents

SUMMARY OF CODE DEVELOPMENT	3
1. FRICTION FORCE IN NONMAGNETIZED ELECTRON BEAM	5
1.1. Numerical calculation of the force components	5
1.2. Asymptotic representation	8
1.3. Benchmarking the code	10
1.4. Modeling of Recycler cooling system	13
2. MODELS OF ELECTRON COOLING FRICTION FORCE	17
2.1. Formula by Erlangen Univ.	17
2.2. 3D non-magnetized friction force	19
2.3. Electron beam as an array of particles	21
2.4. Real distribution of electrons	24
2.5. Electron beam shifts and painting procedure	28
3. STOCHASTIC COOLING SIMULATION	31
3.1. Cooling rate calculation	31
3.2. Power consumption	33
3.3. Kick of the ion momentum components due to action of stochastic cooling	35
4. OPTICAL STOCHASTIC COOLING	41
5. DEVELOPMENT OF KINETIC MODELS FOR IBS AND ECOOL	43
5.1. Kinetic model of IBS on the basis of Bjorken-Mtingwa theory	43
5.2. Benchmarking of the kinetic model	48
5.3. Friction and diffusion in the array of particles	49
5.4. Simulation of diffusion processes in model beam	50
REFERENCES	54

SUMMARY OF CODE DEVELOPMENT

Initial design of RHIC electron cooling system presumed generation of the magnetized electron beam with the cooling section solenoid providing the longitudinal magnetic field of 2 – 5 T. A large emittance of the electron beam used in this approach prevents ion-electron recombination in the cooling section while an electron magnetization provides the cooling force needed.

A few models for magnetized cooling simulation were developed under the previous contracts between BNL and JINR. The results of the magnetized friction force calculation were compared with simulation of ion dynamics in an electron cloud using VORPAL code and with dedicated experiments at CELSIUS cooling system. As a result, the accuracy of the magnetized cooling rate calculation was substantially increased. Simulations showed that for sufficient increase of the luminosity in RHIC based on the magnetized approach a required charge of the electron bunch should be about 20 nC.

Electron cooling in RHIC based on the non-magnetized electron beam sufficiently simplifies the cooler design. Generation and acceleration of the electron bunch without longitudinal magnetic field permits to reach low value of emittance in the cooling section. Suppression of the ion recombination with electrons in the cooling section can be performed using undulator with relatively weak magnetic field $\sim 10\div 50$ G. The cooling rate required for the suppression of intrabeam scattering can be obtained with relatively small charge of the electron bunch $\sim 2\div 5$ nC.

Obvious advantages of the non-magnetized version of the cooler design stimulated development and benchmarking of the algorithms for the cooling force calculation in the absence of the magnetic field. In previous version of BETACOOOL program the following algorithms were used for the non-magnetized friction force:

- numerical evaluation of 3D integral over the electron distribution function in the case of flattened velocity distribution,
- Chandrasekhar's formula for the friction force with uniform Maxwellian velocity distribution,
- asymptotic formulae for the friction force with flattened velocity distribution derived by Meshkov.

To provide accurate benchmarking of existing algorithms and to improve accuracy and speed of the calculation two new algorithms were introduced into the code: Binney's formula and asymptotic representation by Derbenev for flattened velocity distribution.

The electron cooling of 8 GeV antiprotons at Recycler cooling system (Fermilab) commissioned in 2005, can be referred to as the "non-magnetized". To provide comparison between the friction force simulated with BETACOOOL and the cooling rate measured at Recycler, the algorithm for direct simulation of the evolution of the ion beam parameters during a voltage step procedure was introduced into the code.

Binary collision model for the friction force derived by Erlangen Univ. (Germany) was implemented in the program. The results of the friction force calculation with this program were used for benchmarking of new model of the cooling force in BETACOOOL code.

Numerical algorithm of the cooling force calculation from the real distribution of the electron bunch was developed. The design of new electron gun for the RHIC cooler is realized with PARMELA code. Calculated with PARMELA coordinates and velocities of accelerated electron bunch can be loaded into BETACOOOL code and the cooling process with real electron distribution can be produced.

The designed electron bunch has smaller length than the one of ion beam. For the effective cooling process the special painting procedure of the electron bunch position over the ion beam position is necessary. For the optimization of this process the painting procedure was realized in BETACOOOL code.

To provide more accurate simulations of Intrabeam scattering process the algorithm structure was modified. In the tracking procedure the longitudinal motion representation was corrected and tested. The modules for particle coordinate transformation from laboratory frame to beam frame and back were introduced. To avoid significant increase in simulation time the possibility to change an integration step over time for each process independently was introduced.

Algorithm for the optical stochastic cooling simulation developed by BNL was implemented into the code. For simulation of usual stochastic cooling the model developed by FZJ (Juelich, Germany) can be used in present the simulations. Description of this algorithm is also included in this report.

In the last chapter we describe the realized and benchmarked simplified kinetic model of the IBS process, the algorithm realized for calculation of the friction and diffusion acting on the ion in the electron beam presented as an array of particles, the structure of developed algorithms for Langevin force calculation with general form of the diffusion tensor and for kinetic IBS simulation using local array of the ions.

1. FRICTION FORCE IN NONMAGNETIZED ELECTRON BEAM

1.1. Numerical calculation of the force components

In the particle rest frame the friction force acting on the ion at charge number Z inside a nonmagnetized electron beam at density of n_e can be evaluated by numerical integration of the following formula

$$\vec{F} = -\frac{4\pi n_e e^4 Z^2}{m} \int \ln\left(\frac{\rho_{\max}}{\rho_{\min}}\right) \frac{\vec{V} - \vec{v}_e}{|\vec{V} - \vec{v}_e|^3} f(v_e) d^3 v_e, \quad (1.1)$$

where e and m are the electron charge and mass, V and v_e are the ion and electron velocities respectively.

The Coulomb logarithm $\ln\frac{\rho_{\max}}{\rho_{\min}}$ is kept under the integral because the minimal impact parameter depends on electron velocity:

$$\rho_{\min} = \frac{Ze^2}{m} \frac{1}{|\vec{V} - \vec{v}_e|^2}. \quad (1.2)$$

At given value of the ion velocity the maximum impact parameter is constant and it is determined by dynamic shielding radius or the ion time of flight through the electron cloud. Radius of the dynamic shielding sphere coincides with Debye radius:

$$\rho_D = \frac{\Delta_e}{\omega_p}, \quad (1.3)$$

when the ion velocity is less than the electron velocity spread Δ_e . The plasma frequency ω_p is equal to

$$\omega_p = \sqrt{\frac{4\pi n_e e^2}{m}}. \quad (1.4)$$

When the ion velocity sufficiently larger than the electron velocity spread it determines the shielding radius

$$\rho_{sh} = \frac{V}{\omega_p}. \quad (1.5)$$

The both formulae (1.3) and (1.5) can be combined together to have a smooth dependence of the shielding radius on the ion velocity:

$$\rho_{sh} = \frac{\sqrt{V^2 + \Delta_e^2}}{\omega_p}. \quad (1.6)$$

In the case, when the shielding sphere does not contain big enough number of electrons to compensate the ion charge (such a situation takes a place in the case of magnetized electron beam at low longitudinal velocity spread) it has to be increased in accordance with the electron beam density and the ion charge. In the program this radius is estimated from the expression

$$n_e \rho^3 \sim 3Z. \quad (1.7)$$

As a result, the maximum impact parameter is calculated as a minimum from three values:

$$\rho_{\max} = \min \left\{ \max \left(\rho_{sh}, \sqrt[3]{\frac{3Z}{n_e}} \right), V\tau \right\}. \quad (1.8)$$

The second term describes the distance, which the ion passes inside the electron beam. Here τ is the ion time of flight the cooling section in the PRF:

$$\tau = \frac{l_{cool}}{\beta\gamma c}. \quad (1.9)$$

In the case of axial symmetry the electron distribution function can be written in the following form:

$$f(v_e) = \left(\frac{1}{2\pi} \right)^{3/2} \frac{1}{\Delta_{\perp}^2 \Delta_{\parallel}} \exp \left(-\frac{v_{\perp}^2}{2\Delta_{\perp}^2} - \frac{v_{\parallel}^2}{2\Delta_{\parallel}^2} \right), \quad (1.10)$$

where Δ_{\perp} and Δ_{\parallel} are the electron velocity spreads in the transverse and longitudinal direction correspondingly. The shielding cloud in this case has an ellipsoidal shape which can be approximated by the sphere of radius calculated using effective electron velocity spread:

$$\Delta_e^2 = \Delta_{\perp}^2 + \Delta_{\parallel}^2. \quad (1.11)$$

The components of the friction force (1.1) can be calculated in cylindrical co-ordinate system as follows:

$$F_{\perp} = -\sqrt{\frac{2}{\pi}} \frac{Z^2 e^4 n_e}{m \Delta_{\perp}^2 \Delta_{\parallel}} \int_0^{\infty} \int_{-\infty}^{\infty} \int_0^{2\pi} \ln \left(\frac{\rho_{\max}}{\rho_{\min}} \right) \frac{(V_{\perp} - v_{\perp} \cos \varphi) \exp \left(-\frac{v_{\perp}^2}{2\Delta_{\perp}^2} - \frac{v_{\parallel}^2}{2\Delta_{\parallel}^2} \right)}{\left((V_{\parallel} - v_{\parallel})^2 + (V_{\perp} - v_{\perp} \cos \varphi)^2 + v_{\perp}^2 \sin^2 \varphi \right)^{3/2}} v_{\perp} d\varphi dv_{\parallel} dv_{\perp},$$

$$F_{\parallel} = -\sqrt{\frac{2}{\pi}} \frac{Z^2 e^4 n_e}{m \Delta_{\perp}^2 \Delta_{\parallel}} \int_0^{\infty} \int_{-\infty}^{\infty} \int_0^{2\pi} \ln \left(\frac{\rho_{\max}}{\rho_{\min}} \right) \frac{(V_{\parallel} - v_{\parallel}) \exp \left(-\frac{v_{\perp}^2}{2\Delta_{\perp}^2} - \frac{v_{\parallel}^2}{2\Delta_{\parallel}^2} \right)}{\left((V_{\parallel} - v_{\parallel})^2 + (V_{\perp} - v_{\perp} \cos \varphi)^2 + v_{\perp}^2 \sin^2 \varphi \right)^{3/2}} v_{\parallel} d\varphi dv_{\parallel} dv_{\perp}.$$

(1.12)

Within an accuracy of about 2% the upper limit of the integrals over velocity components can be replaced from infinity to three corresponding rms values and integration over φ can be performed from 0 to π due to symmetry of the formulae. In this case the friction force components can be calculated as:

$$\begin{aligned}
F_{\perp} &= -\frac{4\pi Z^2 e^4 n_e}{m \cdot \text{Int}} \int_0^{3\Delta_{\perp}} \int_{-3\Delta_{\parallel}}^{3\Delta_{\parallel}} \int_0^{\pi} \ln\left(\frac{\rho_{\max}}{\rho_{\min}}\right) \frac{(V_{\perp} - v_{\perp} \cos \varphi) \exp\left(-\frac{v_{\perp}^2}{2\Delta_{\perp}^2} - \frac{v_{\parallel}^2}{2\Delta_{\parallel}^2}\right)}{\left((V_{\parallel} - v_{\parallel})^2 + (V_{\perp} - v_{\perp} \cos \varphi)^2 + v_{\perp}^2 \sin^2 \varphi\right)^{3/2}} v_{\perp} d\varphi dv_{\parallel} dv_{\perp}, \\
F_{\parallel} &= -\frac{4\pi Z^2 e^4 n_e}{m \cdot \text{Int}} \int_0^{3\Delta_{\perp}} \int_{-3\Delta_{\parallel}}^{3\Delta_{\parallel}} \int_0^{\pi} \ln\left(\frac{\rho_{\max}}{\rho_{\min}}\right) \frac{(V_{\parallel} - v_{\parallel}) \exp\left(-\frac{v_{\perp}^2}{2\Delta_{\perp}^2} - \frac{v_{\parallel}^2}{2\Delta_{\parallel}^2}\right)}{\left((V_{\parallel} - v_{\parallel})^2 + (V_{\perp} - v_{\perp} \cos \varphi)^2 + v_{\perp}^2 \sin^2 \varphi\right)^{3/2}} v_{\perp} d\varphi dv_{\parallel} dv_{\perp},
\end{aligned}
\tag{1.13}$$

where the normalization factor is calculated in accordance with:

$$\text{Int} = \int_0^{3\Delta_{\perp}} \int_{-3\Delta_{\parallel}}^{3\Delta_{\parallel}} \int_0^{\pi} \exp\left(-\frac{v_{\perp}^2}{2\Delta_{\perp}^2} - \frac{v_{\parallel}^2}{2\Delta_{\parallel}^2}\right) v_{\perp} d\varphi dv_{\parallel} dv_{\perp}. \tag{1.14}$$

The minimal impact parameter is the following function of the electron velocity components:

$$\rho_{\min} = \frac{Ze^2}{m_e} \frac{1}{(V_{\parallel} - v_{\parallel})^2 + (V_{\perp} - v_{\perp} \cos \varphi)^2 + v_{\perp}^2 \sin^2 \varphi}. \tag{1.15}$$

At the ion velocity $V \gg \Delta_{\parallel}, \Delta_{\perp}$ the minimal impact parameter becomes to be constant:

$$\rho_{\min} = \frac{Ze^2}{m_e} \frac{1}{V_{\perp}^2 + V_{\parallel}^2}, \tag{1.16}$$

and Coulomb logarithm can be removed from the integral. At extremely small ion velocity the calculation of the minimal impact parameter in accordance with the formula (1.16) leads to zero friction force value, when becomes to be $\rho_{\min} > \rho_{\max}$. One can avoid this problem introducing mean minimal impact parameter in accordance with

$$\rho_{\min} = \frac{Ze^2}{m_e} \frac{1}{V_{\perp}^2 + V_{\parallel}^2 + \Delta_{\perp}^2 + \Delta_{\parallel}^2}. \tag{1.17}$$

When the Coulomb logarithm L_C is constant the two of three integrals in (1.12) can be calculated analytically and the friction force components can be written in accordance with Binney's formulae:

$$\begin{aligned}
F_{\perp} &= 2\sqrt{2\pi} \frac{n_e e^4 Z^2 L_C}{m} \frac{V_{\perp}}{\Delta_{\perp}^3} B_{\perp} \\
F_{\parallel} &= 2\sqrt{2\pi} \frac{n_e e^4 Z^2 L_C}{m} \frac{V_{\parallel}}{\Delta_{\perp}^3} B_{\parallel},
\end{aligned} \tag{1.19}$$

where B_{\perp} and B_{\parallel} are the following integrals:

$$\begin{aligned}
B_{\perp} &= \int_0^{\infty} \frac{\exp\left(-\frac{V_{\perp}^2}{2\Delta_{\perp}^2} \frac{1}{1+q} - \frac{V_{\parallel}^2}{2\Delta_{\perp}^2} \frac{1}{(\Delta_{\parallel}/\Delta_{\perp})^2 + q}\right)}{(1+q)^2 \left((\Delta_{\parallel}/\Delta_{\perp})^2 + q\right)^{1/2}} dq, \\
B_{\parallel} &= \int_0^{\infty} \frac{\exp\left(-\frac{V_{\perp}^2}{2\Delta_{\perp}^2} \frac{1}{1+q} - \frac{V_{\parallel}^2}{2\Delta_{\perp}^2} \frac{1}{(\Delta_{\parallel}/\Delta_{\perp})^2 + q}\right)}{(1+q) \left((\Delta_{\parallel}/\Delta_{\perp})^2 + q\right)^{3/2}} dq.
\end{aligned} \tag{1.20}$$

In the case of uniform Maxwellian distribution (when $\Delta_{\parallel} = \Delta_{\perp} = \Delta_e$) the integrals (1.20) coincide with each other and reproduce Chandrasekhar's formula. In Budker's notation it has the following form:

$$\begin{aligned}
\vec{F} &= -\frac{\vec{V}}{V^3} \frac{4\pi m_e e^4 Z^2 L_C}{m} \varphi\left(\frac{V}{\Delta_e}\right), \text{ where} \\
\varphi(x) &= \sqrt{\frac{2}{\pi}} \int_0^x e^{-y^2/2} dy - \sqrt{\frac{2}{\pi}} x e^{-x^2/2}.
\end{aligned} \tag{1.21}$$

The formulae (1.12) have to give the same result when the logarithm is removed from the integrals.

1.2. Asymptotic representation

For fast simulation of the cooling process in the BETACOOl were used asymptotic formulae derived by I. Meshkov. In the case, when transverse velocity spread of electrons is substantially larger than longitudinal one the friction force components are approximated in three ranges of the ion velocity.

I. High velocity $V \geq \Delta_{\perp}$, here longitudinal and transverse components of the friction force are equal:

$$\vec{F} = -\frac{4\pi Z^2 e^4 n_e L_C}{m} \frac{\vec{V}}{V^3}, \tag{1.22}$$

and in this range the friction force shape coincides with formula (1.21).

II. Low velocity $\Delta_{\parallel} \leq V < \Delta_{\perp}$. Here the transverse component of the friction force is given by the following expression:

$$F_{\perp} = -\frac{4\pi Z^2 e^4 n_e L_C}{m} \cdot \frac{V_{\perp}}{\Delta_{\perp}^3}, \tag{1.23}$$

and longitudinal one:

$$F_{\parallel} = -\frac{4\pi Z^2 e^4 n_e L_C}{m} \frac{V_{\parallel}}{|V_{\parallel}| \Delta_{\perp}^2}. \tag{1.24}$$

III. Superlow velocity $V < \Delta_{\parallel}$. Here the transverse component of the friction force is equal to zero, the longitudinal component is given by:

$$F_{\parallel} = -\frac{4\pi Z^2 e^4 n_e L_C}{m} \frac{V_{\parallel}}{\Delta_{\parallel} \Delta_{\perp}^2}. \quad (1.25)$$

The minimal impact parameter in the Coulomb logarithm is equal to:

$$\rho_{\min} = \frac{Ze^2}{m} \frac{1}{V^2 + \Delta_e^2}. \quad (1.26)$$

For the longitudinal component of the friction force at zero transverse velocity the asymptotic formulae was derived by Ya. Derbenev in the following form:

$$F_{\parallel} = -\frac{4\pi Z^2 e^4 n_e L(V_{\parallel})}{m} \frac{V_{\parallel}}{\Delta_{\parallel} \Delta_{\perp}^2} \sqrt{\frac{2}{\pi}}, \text{ if } V \ll \Delta_{\parallel}. \quad (1.27)$$

$$F_{\parallel} = -\frac{4\pi Z^2 e^4 n_e}{m} \left[L(V_{\parallel}) \frac{V_{\parallel}}{|V_{\parallel}| \Delta_{\perp}^2} - \sqrt{\frac{\pi}{2}} L(\Delta_{\perp}) \frac{V_{\parallel}}{\Delta_{\perp}^3} \right], \text{ if } \Delta_{\perp} > V \gg \Delta_{\parallel}. \quad (1.28)$$

Here the Coulomb logarithms are calculated in accordance with the following formulae:

$$L(V_{\parallel}) = \ln \left(\sqrt{\frac{V_{\parallel}^2 m}{4\pi m_e e^2}} / \rho_{\min} \right), \quad (1.29)$$

$$L(\Delta_{\perp}) = \ln \left(\sqrt{\frac{\Delta_{\perp}^2 m}{4\pi m_e e^2}} / \rho_{\min} \right). \quad (1.30)$$

In order to provide uniform usage of the formulae in the program the friction force calculation was realized in three ranges of the ion velocity similarly to Meshko's asymptotes.

I. High velocity $V \geq \Delta_{\perp}$, here longitudinal and transverse components of the friction force are equal:

$$F_{\perp} = -\frac{4\pi Z^2 e^4 n_e L_C}{m} \frac{V_{\perp}}{V^3}, \quad (1.31)$$

$$F_{\parallel} = -\frac{4\pi Z^2 e^4 n_e}{m} \left(L_C \frac{V_{\parallel}}{V^3} - \sqrt{\frac{2}{\pi}} L(\Delta_{\perp}) \frac{1}{V_{\parallel}^2} \right). \quad (1.32)$$

II. Low velocity $\Delta_{\parallel} \leq V < \Delta_{\perp}$. Here the transverse component of the friction force is given by the following expression:

$$F_{\perp} = -\frac{4\pi Z^2 e^4 n_e L_C}{m} \frac{V_{\perp}}{\Delta_{\perp}^3}, \quad (1.33)$$

and longitudinal one:

$$F_{\parallel} = -\frac{4\pi Z^2 e^4 n_e}{m} \left(L_c \frac{V_{\parallel}}{\sqrt{V_{\parallel}^2 + \Delta_{\parallel}^2 \Delta_{\perp}^2}} - \sqrt{\frac{2}{\pi}} L(\Delta_{\perp}) \frac{V_{\parallel}}{\Delta_{\perp}^3} \right). \quad (1.34)$$

III. Superlow velocity $V < \Delta_{\parallel}$. Here the transverse component of the friction force is equal to zero, the longitudinal component is given by:

$$F_{\parallel} = -\frac{4\pi Z^2 e^4 n_e}{m} L_c \frac{V_{\parallel}}{\sqrt{V_{\parallel}^2 + \Delta_{\parallel}^2 \Delta_{\perp}^2}}. \quad (1.35)$$

These formulae in the case $V_{\perp} = 0$ give the correct result for longitudinal component of the friction force (1.27), (1.28) and have a correct asymptotes at high ion velocity. The transverse component of the force is calculated in accordance with Meshkov's representation.

1.3. Benchmarking the code

All the formulae for the numerical friction force calculation (1.12, 1.19 and 1.21) have to coincide in the case of uniform Maxwellian distribution of the electrons if the Coulomb logarithm is moved under the integral. In this case the friction is symmetrical in the transverse and longitudinal degrees of freedom. The formulae were tested at Recycler cooling system parameters that are listed in the Table 1.1.

Table 1. The cooling system parameters used in simulations.

Cooling section length, m	20
Electron energy, MeV	4.36
Beta functions in the cooling section, m	20
Electron current, A	0.2
Electron beam radius, cm	0.45
Transverse temperature, eV	0.5
Longitudinal temperature, eV	0.01

In the Fig. 1.1. the results of the calculations at $T_{\parallel} = T_{\perp} = 0.5$ eV using different formulae are presented.

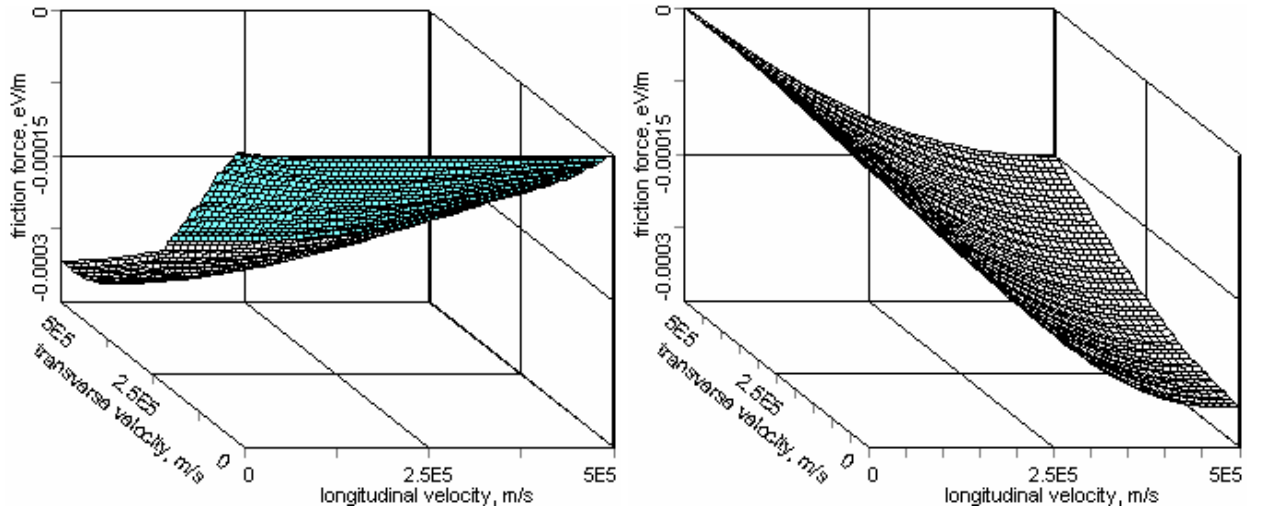


Fig. 1.1, a. Friction force components (left plot - transverse, right plot – longitudinal) as functions of the ion velocity calculated with Chandrasekhar's formula.

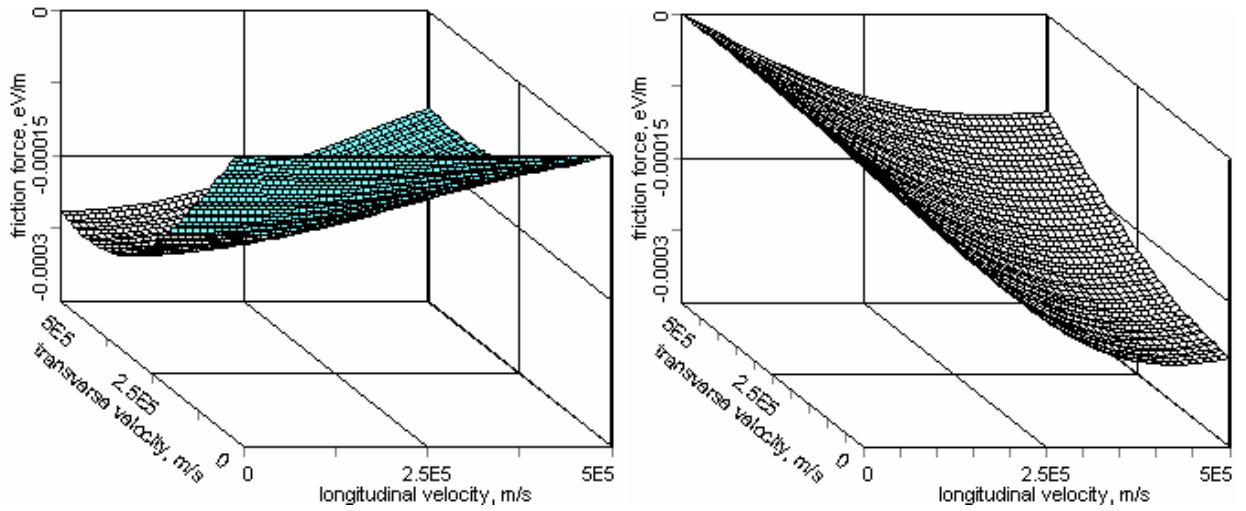


Fig. 1.1, b. Friction force components (left plot - transverse, right plot – longitudinal) as functions of the ion velocity calculated with Binney's formula. Integration step is 0.003, upper limit is 3.

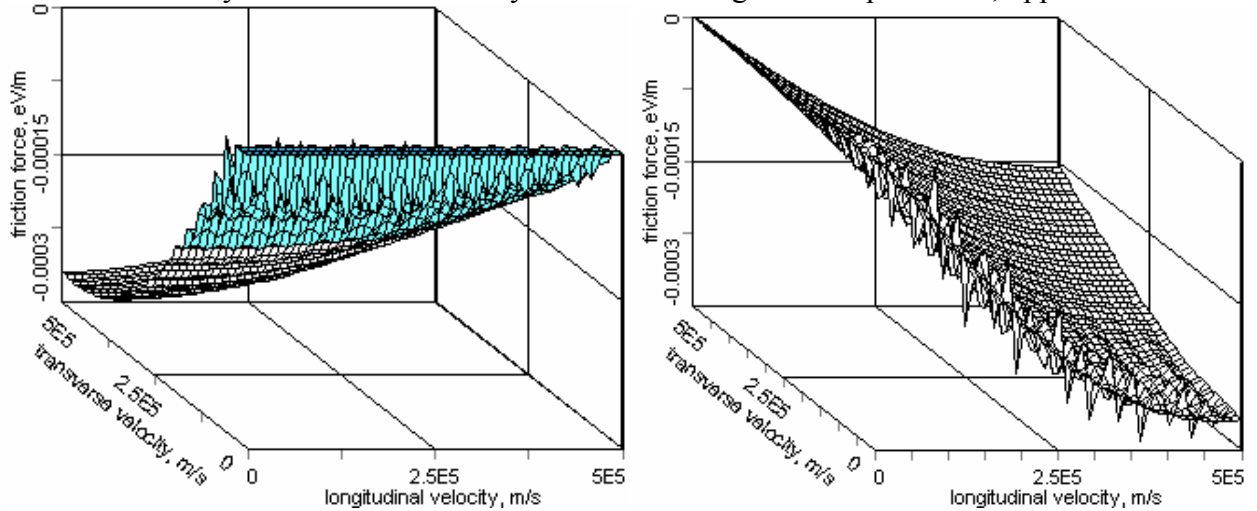


Fig. 1.1, c. Friction force components (left plot - transverse, right plot – longitudinal) as functions of the ion velocity calculated by numerical evaluation of 3D integral (1.13). The Coulomb logarithm is removed from the integral. Number of integration steps over the transverse velocity is 27, over the longitudinal velocity - 26, over the angle - 15.

The maximum position and amplitude of the friction force calculated using different formulae coincide within the accuracy of numerical integration. The numerical evaluation of 3D integral requires by about 100 times longer calculation time and the accuracy decreases in the region of small velocity (one can see a numerical noise in the Fig. 1.1, b due to small number of the integration steps). The numerical noise in the region of small ion velocity at evaluation of 3D integral is sufficiently less, when the Coulomb logarithm is kept under the integral.

At flattened electron velocity distribution the Binney's formula has to coincide with the numerical evaluation of 3D integral (1.13) when the Coulomb logarithm is removed over the integral. In the Fig 1.2 the results of the force calculation at $T_{\parallel} = 0.01$ eV are presented. At the flattened velocity distribution the amplitude of the longitudinal component of the friction force is larger than the transverse one, and the maximum position is located near the electron longitudinal velocity spread. Both the formulae give the same result with the accuracy of numerical integration.

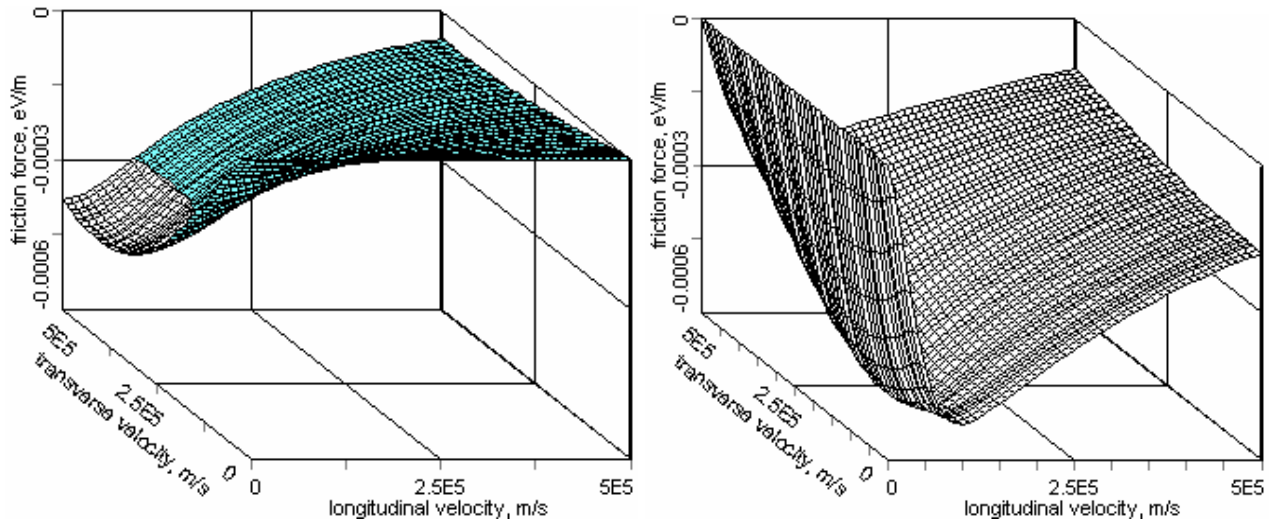


Fig. 1.2, a. Friction force components (left plot - transverse, right plot – longitudinal) as functions of the ion velocity calculated with Biney's formula. Integration step is 0.003, upper limit is 3.

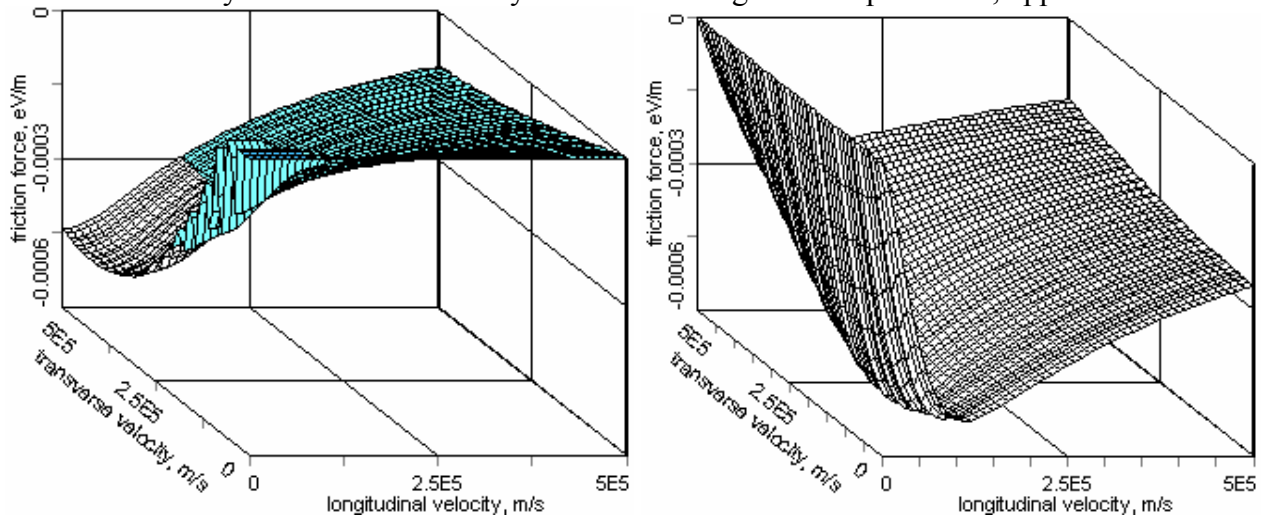


Fig. 1.2, b. Friction force components (left plot - transverse, right plot – longitudinal) as functions of the ion velocity calculated by numerical evaluation of 3D integral (1.13). The Coulomb logarithm is removed from the integral. Number of integration steps over the transverse velocity is 27, over the longitudinal velocity - 26, over the angle - 15.

The difference in the friction forces calculated as a 3D integral with Coulomb logarithm inside or outside the integral is illustrated in the Fig. 1.3.

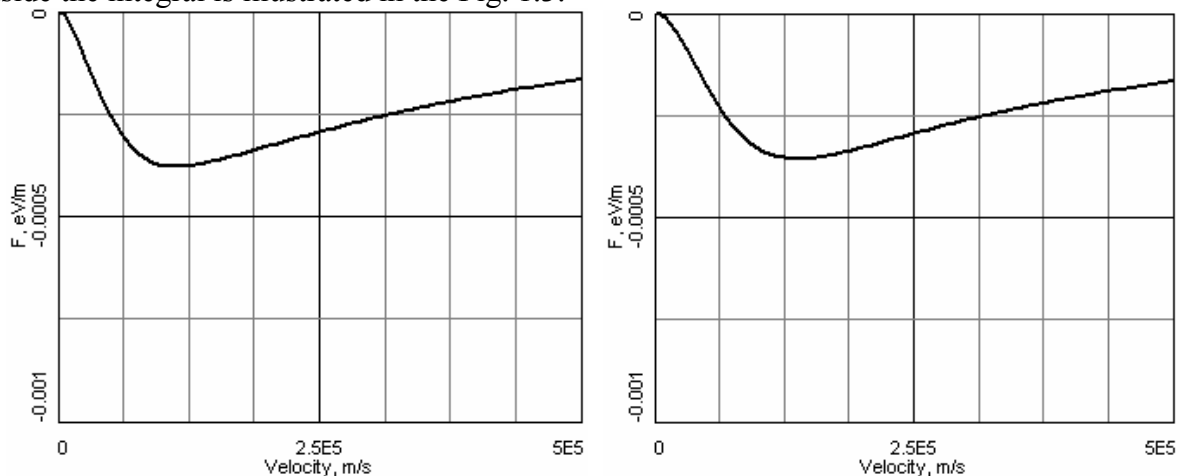


Fig. 1.3. The longitudinal component of the friction force as function of longitudinal ion velocity. Coulomb logarithm is removed from the integral - left plot, coulomb logarithm is under the integral – right plot.

One can see that the accurate treatment of the Coulomb logarithm leads to slight decrease of the friction force value and displacement of the maximum position into the region of larger ion velocity. It means that at used parameters of the cooler the Binney's formula provide good enough accuracy of the calculation at sufficiently less calculation time. At other cooler parameters the numerical evaluation of 3D integral can be used for estimation of the accuracy of other formulae and for simulations can be used more fast algorithm.

For comparison between numerical and asymptotic representations of the friction force the longitudinal component of the force calculated in accordance with Meshkov's formulae is shown in the Fig. 1.4. One can see that this asymptote sufficiently overestimate the friction force and it can be used only for very rough estimates.

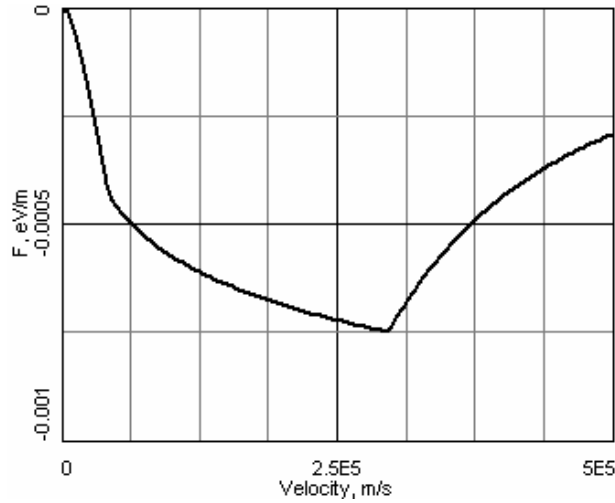


Fig. 1.4. Meshkov's asymptote of the friction force longitudinal component.

More appropriate candidate for comparison of the numerical results of the friction force calculation with experiments is Recycler cooling system realizing the nonmagnetized cooling of antiprotons. To simplify the comparison a few modifications in the program were done.

1.4. Modeling of Recycler cooling system

At usual electron cooling systems a longitudinal magnetic field is used for transportation of the electron beam. At decrease of the magnetic field value in a cooling section the beam quality fast decreases and investigation of nonmagnetized regime of the electron cooling can not be provided in well controlled conditions. In July 2005 the Recycler cooling system was put into operation in Fermilab. At this cooling system the longitudinal magnetic field in the cooling section is used only to preserve angular spread of electrons θ at the level below 200 μrad . The required longitudinal magnetic field value B is 105 G that corresponds to electron rotation with Larmor radius

$$\rho_{\perp} = \frac{pc}{eB} \theta \approx 3 \cdot 10^{-4} m,$$

where $pc = 4,85$ MeV is the electron momentum. The cooling section length is 20 m which approximately corresponds to 2 steps of the Larmor helix. Maximum impact parameter at maximum electron current of 500 mA is restricted by time of flight the cooling section and it is equal

$$\rho_{\max} \approx 7 \cdot 10^{-5} m,$$

that is smaller than the electron Larmor radius. At such parameters one can expect, that the impact of magnetized collisions into the friction force is negligible.

To provide accurate comparison between results of experimental investigations at Recycler and numerical simulation with BETACOOOL a few new algorithms were implemented and tested. General method for friction force measurements at Recycler is Voltage Step method and general attention was devoted to simulation of this procedure in BETACOOOL.

One of the peculiarities of the Recycler cooling system is sufficient dependence of the electron transverse velocity spread on the distance from the beam centre. This effect appears due to the beam envelope mismatch with the transportation channel. In the first approximation this effect can be presented as a linear increase of the velocity spread with radial co-ordinate:

$$\Delta_{\perp} = \frac{d\Delta_{\perp}}{dr} r, \quad (1.36)$$

where the velocity gradient $\frac{d\Delta_{\perp}}{dr}$ is input into the simulations as an additional parameter of the electron beam (last parameter in the Fig. 1.5).

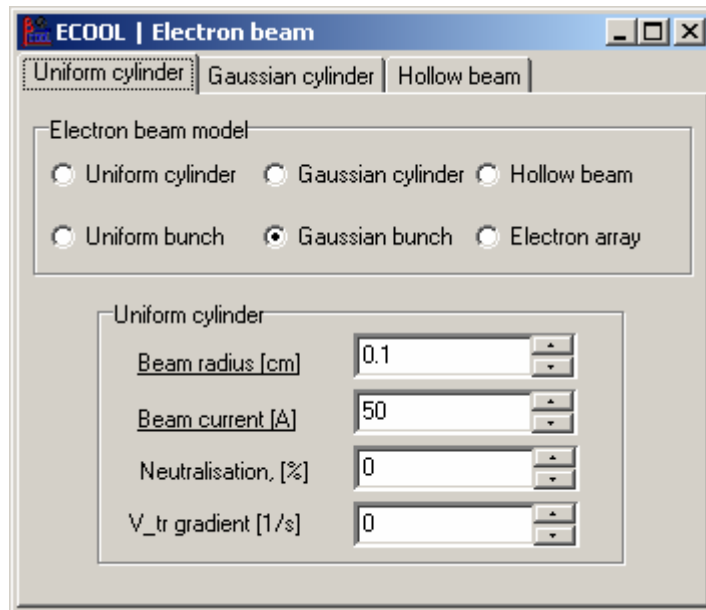


Fig. 1.5. Modification of the visual form for input a transverse velocity gradient.

To simulate the High Voltage step in the electron cooler the electron momentum can be varied during simulations by change of the parameter “dP/P shift” (Fig. 1.5). RMS dynamics simulation presumes that the mean ion momentum is constant during evolution therefore the voltage step method can be simulated only in the frame of Model Beam algorithm. The mean momentum of the ions is output in additional curve “dpmo2t.cur” and can be visualized in the same plot with a momentum spread in the corresponding form of the Windows interface.

An example of the cooling process simulation is presented in the Fig. 1.6. The red curve correspond to mean antiproton momentum. The first 1700 sec correspond to preliminary cooling of antiprotons. At 1700 sec the electron momentum was shifted by the relative value of 10^{-3} and during next 2000 sec the mean antiproton momentum is cooled to the new momentum of the electrons. The green curve presents the variation in time of the antiproton momentum spread.

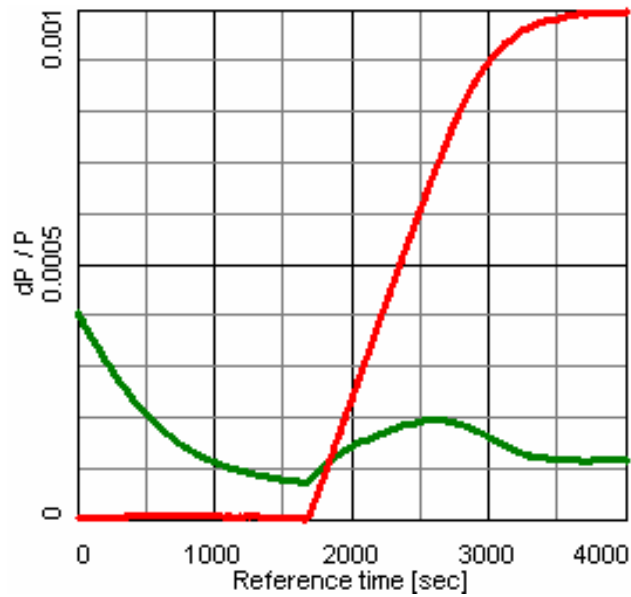


Fig. 1.6. Simulation of the voltage step method using BETACOOOL program. The electron beam parameters are presented in the Table 1.1.

Evolution of the antiproton momentum during the friction force measurement is also output as a 3D plot of the profile versus time as shown in the Fig 1.7.

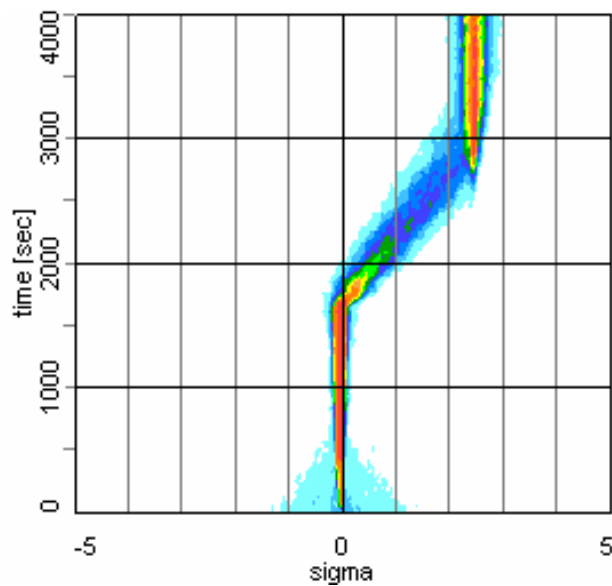


Fig. 1.7. The longitudinal profile evolution during friction force measurement.

To reproduce the procedure using in Fermilab for the beam longitudinal distribution measurement the possibility to average of a few consequent longitudinal profiles was introduced. An example of a few consequent averaged profiles calculated with BETACOOOL after 2 keV step of the electron energy is presented in the Fig. 1.8. The electron beam current is 500 mA.

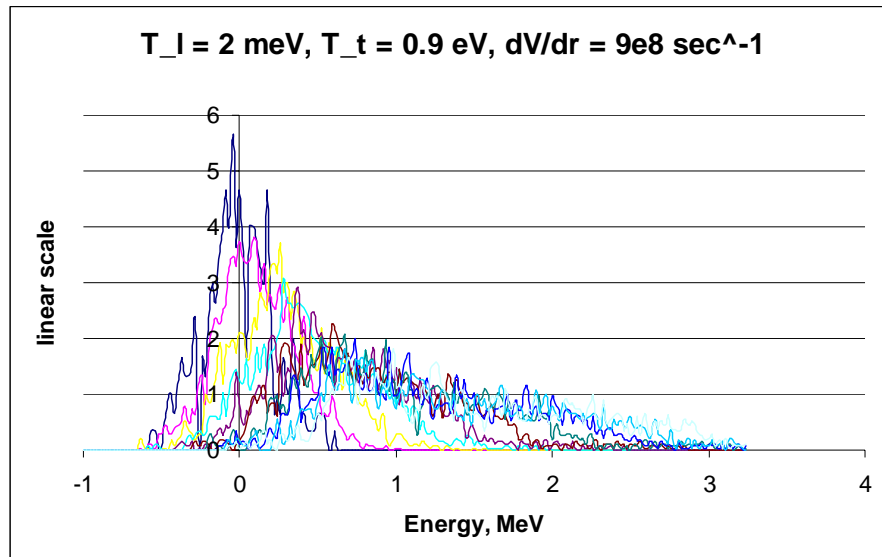


Fig. 1.8. Evolution of the longitudinal profile in time. Distance between slices is 50 sec.

2. MODELS OF ELECTRON COOLING FRICTION FORCE

2.1. Formula by Erlangen Univ.

In [C.Toepffer et al., Erlangen Univ.] the friction force was calculated in the frame of binary collision model under assumption that the ion velocity stays constant in a collision with an electron. The unperturbed motion of electron is a helix with the Larmor radius:

$$\rho_{\perp} = \frac{cmv_{\perp}}{eB} \quad (2.1)$$

and the pitch determined by longitudinal velocity. The ion velocity variation is calculated iteratively and at impact parameters larger than the Larmor radius one can obtain solution in a closed form for two limiting cases:

$$\delta = \frac{cm\sqrt{V_{\perp}^2 + (V_{\parallel} - v_{\parallel})^2}}{eB} \gg \rho_{\perp}$$

and $\delta \ll \rho_{\perp}$

where δ is the pitch of the helix as seen from the ion.

Correspondingly, the friction force includes three components related to different types of collision:

- fast collisions at impact parameters less than radius of electron rotation,
- collisions with “tight” helices,
- collisions with “stretched” helices.

In the case of axial symmetry the electron distribution function can be written in the following form:

$$f(v_e) = \left(\frac{1}{2\pi}\right)^{3/2} \frac{1}{\Delta_{\perp}^2 \Delta_{\parallel}} \exp\left(-\frac{v_{\perp}^2}{2\Delta_{\perp}^2} - \frac{v_{\parallel}^2}{2\Delta_{\parallel}^2}\right), \quad (2.2)$$

where Δ_{\perp} and Δ_{\parallel} are the electron rms velocity spreads in the transverse and longitudinal direction correspondingly.

For the fast collisions the formula is analogous to non-magnetized collisions. The components of the friction force at fast collisions can be calculated in cylindrical co-ordinate system as follows:

$$F_{\perp,f} = -\sqrt{\frac{2}{\pi}} \frac{Z^2 e^4 n_e}{m \Delta_{\perp}^2 \Delta_{\parallel}} \int_0^{\infty} \int_{-\infty}^{\infty} \int_0^{2\pi} \ln\left(\frac{\rho_{\max}}{\rho_{\min}}\right) \frac{(V_{\perp} - v_{\perp} \cos \varphi) \exp\left(-\frac{v_{\perp}^2}{2\Delta_{\perp}^2} - \frac{v_{\parallel}^2}{2\Delta_{\parallel}^2}\right)}{\left((V_{\parallel} - v_{\parallel})^2 + (V_{\perp} - v_{\perp} \cos \varphi)^2 + v_{\perp}^2 \sin^2 \varphi\right)^{3/2}} v_{\perp} d\varphi dv_{\parallel} dv_{\perp},$$

$$F_{\parallel,f} = -\sqrt{\frac{2}{\pi}} \frac{Z^2 e^4 n_e}{m \Delta_{\perp}^2 \Delta_{\parallel}} \int_0^{\infty} \int_{-\infty}^{\infty} \int_0^{2\pi} \ln\left(\frac{\rho_{\max}}{\rho_{\min}}\right) \frac{(V_{\parallel} - v_{\parallel}) \exp\left(-\frac{v_{\perp}^2}{2\Delta_{\perp}^2} - \frac{v_{\parallel}^2}{2\Delta_{\parallel}^2}\right)}{\left((V_{\parallel} - v_{\parallel})^2 + (V_{\perp} - v_{\perp} \cos \varphi)^2 + v_{\perp}^2 \sin^2 \varphi\right)^{3/2}} v_{\perp} d\varphi dv_{\parallel} dv_{\perp}. \quad (2.3)$$

But here both impact parameters – minimum and maximum – are the functions of the electron velocity:

$$\rho_{\min} = \frac{Ze^2}{m_e} \frac{1}{(V_{\parallel} - v_{\parallel})^2 + (V_{\perp} - v_{\perp} \cos \varphi)^2 + v_{\perp}^2 \sin^2 \varphi}. \quad (2.4)$$

$$\rho_{\max} = \rho_{\perp} = \frac{cmv_{\perp}}{eB}.$$

The friction force in collisions with tight helices

$$F_{\parallel,t}(V_{\perp}, V_{\parallel}) = -\frac{4\pi Z^2 e^4 n_e}{m} \frac{1}{\Delta_{\perp}^2 \sqrt{2\pi} \Delta_{\parallel}} \int \frac{V_{\perp}^2 (V_{\parallel} - v_{\parallel})}{(V_{\perp}^2 + (V_{\parallel} - v_{\parallel})^2)^{5/2}} \exp\left(-\frac{v_{\parallel}^2}{2\Delta_{\parallel}^2}\right) \int_0^{\infty} \ln\left(\frac{\rho_{\max}}{\max(\rho_{\perp}, \delta)}\right) \exp\left(-\frac{v_{\perp}^2}{2\Delta_{\perp}^2}\right) v_{\perp} dv_{\perp} dv_{\parallel}, \quad (2.5)$$

$$F_{\perp,t}(V_{\perp}, V_{\parallel}) = -\frac{4\pi Z^2 e^4 n_e}{m} \frac{1}{\Delta_{\perp}^2 \sqrt{2\pi} \Delta_{\parallel}} \int \frac{V_{\perp} (V_{\perp}^2 - (V_{\parallel} - v_{\parallel})^2)}{2(V_{\perp}^2 + (V_{\parallel} - v_{\parallel})^2)^{5/2}} \exp\left(-\frac{v_{\parallel}^2}{2\Delta_{\parallel}^2}\right) \int_0^{\infty} \ln\left(\frac{\rho_{\max}}{\max(\rho_{\perp}, \delta)}\right) \exp\left(-\frac{v_{\perp}^2}{2\Delta_{\perp}^2}\right) v_{\perp} dv_{\perp} dv_{\parallel}, \quad (2.6)$$

where

$$\delta = \frac{cm\sqrt{V_{\perp}^2 + (V_{\parallel} - v_{\parallel})^2}}{eB}. \quad (2.7)$$

For stretched helices

$$F_{\parallel,s}(V_{\perp}, V_{\parallel}) = -\frac{4\pi Z^2 e^4 n_e}{m} \frac{1}{\Delta_{\perp}^2 \sqrt{2\pi} \Delta_{\parallel}} \int \frac{V_{\parallel} - v_{\parallel}}{(V_{\perp}^2 + (V_{\parallel} - v_{\parallel})^2)^{3/2}} \exp\left(-\frac{v_{\parallel}^2}{2\Delta_{\parallel}^2}\right) \int_0^{\infty} \ln\left(\frac{\min(\delta, \rho_{\max})}{\min(\rho_{\perp}, \rho_{\max})}\right) \exp\left(-\frac{v_{\perp}^2}{2\Delta_{\perp}^2}\right) v_{\perp} dv_{\perp} dv_{\parallel}, \quad (2.8)$$

$$F_{\perp,s}(V_{\perp}, V_{\parallel}) = -\frac{4\pi Z^2 e^4 n_e}{m} \frac{V_{\perp}}{\Delta_{\perp}^2 \sqrt{2\pi} \Delta_{\parallel}} \int \frac{1}{(V_{\perp}^2 + (V_{\parallel} - v_{\parallel})^2)^{3/2}} \exp\left(-\frac{v_{\parallel}^2}{2\Delta_{\parallel}^2}\right) \int_0^{\infty} \ln\left(\frac{\min(\delta, \rho_{\max})}{\min(\rho_{\perp}, \rho_{\max})}\right) \exp\left(-\frac{v_{\perp}^2}{2\Delta_{\perp}^2}\right) v_{\perp} dv_{\perp} dv_{\parallel}. \quad (2.9)$$

When $V \gg \Delta_{\parallel}$ the electron distribution can be approximated by delta-function $f(v_{\parallel}) = \delta(v_{\parallel})$. In this case integration over electron velocity components can be provided independently. The friction force components for tight helices can be expressed in the following form:

$$F_{\parallel} = -V_{\parallel} \frac{4\pi Z^2 e^4 n_e}{mV^3} \frac{V_{\perp}^2}{V^2} L_M, \quad (2.10)$$

$$F_{\perp} = -V_{\perp} \frac{4\pi Z^2 e^4 n_e L_M}{mV^3} \frac{V_{\perp}^2 - V_{\parallel}^2}{V^2}. \quad (2.11)$$

Here the Coulomb logarithm is determined by the expression

$$L_M = \frac{1}{\Delta_{\perp}^2} \int_0^{\infty} \ln\left(\frac{\rho_{\max}}{\max(\rho_{\perp}, \delta)}\right) \exp\left(-\frac{v_{\perp}^2}{2\Delta_{\perp}^2}\right) v_{\perp} dv_{\perp} \approx \ln\left(\frac{\rho_{\max}}{\langle \rho_{\perp} \rangle}\right),$$

at $\delta = \frac{cm\sqrt{V_{\perp}^2 + V_{\parallel}^2}}{eB}$. Within an accuracy to the logarithm definition these formulae coincide with derived in the limit of infinite magnetic field in [doctoral thesis by V.Parkhomchuk].

In the same approximation $V \gg \Delta_{\parallel}$ the formulae for collisions with stretched helices can be rewritten in the form:

$$\vec{F} \approx -\vec{V} \frac{4\pi Z^2 e^4 n_e}{m} \frac{1}{(V^2 + \Delta_{\parallel}^2)^{3/2}} \left(\ln\left(\frac{\rho_{\max}}{\langle \rho_{\perp} \rangle}\right) + \ln\left(\frac{\omega_p}{\omega_B}\right) \right), \quad (2.12)$$

where ω_p , ω_B are the plasma and cyclotron frequencies. This formula is valid at $\frac{V}{\Delta_{\perp}} \gg 1$ and its structure is similar to semi-empirical formula by Parkhomchuk.

Numerical integration of (5) has to be provided taking into account peculiarity of the integral at $V_{\perp} \rightarrow 0$.

2.2. 3D non-magnetized friction force

In absence of longitudinal magnetic field in the cooling section the electron motion in transverse planes is uncoupled. Correspondingly the electron bunch can has different velocity spreads in horizontal and vertical planes. In this case the friction force can not be presented as a sum of radial and longitudinal components, but it is a vector with all three different components. The components of 3D friction force can be calculated as an integral over electron velocity at given distribution function. In the case of Gaussian electron bunch the distribution function in velocity can be approximated as

$$f(v_e) = \left(\frac{1}{2\pi}\right)^{3/2} \frac{1}{\Delta_x \Delta_y \Delta_{\parallel}} \exp\left(-\frac{v_x^2}{2\Delta_x^2} - \frac{v_y^2}{2\Delta_y^2} - \frac{v_{\parallel}^2}{2\Delta_{\parallel}^2}\right), \quad (2.13)$$

where $\Delta_{x,y,\parallel}$ are the electron velocity spreads in horizontal, vertical and longitudinal planes.

The friction force is calculated in accordance with the definition:

$$\vec{F} = -\sqrt{\frac{2}{\pi}} \frac{Z^2 e^4 n_e}{m \Delta_x \Delta_y \Delta_{\parallel}} \int_{-\infty}^{\infty} \int_{-\infty}^{\infty} \int_{-\infty}^{\infty} \ln\left(\frac{\rho_{\max}}{\rho_{\min}}\right) \frac{(\vec{V} - \vec{v}) \exp\left(-\frac{v_x^2}{2\Delta_x^2} - \frac{v_y^2}{2\Delta_y^2} - \frac{v_{\parallel}^2}{2\Delta_{\parallel}^2}\right)}{\left(\left(V_{\parallel} - v_{\parallel}\right)^2 + (V_x - v_x)^2 + (V_y - v_y)^2\right)^{3/2}} dv_x dv_y dv_{\parallel}, \quad (2.14)$$

where minimum impact parameter is a function of the electron velocity \vec{v} :

$$\rho_{\min} = \frac{Ze^2}{m} \frac{1}{|\vec{V} - \vec{v}|^2}. \quad (2.15)$$

The maximum impact parameter is calculated as usual:

$$\rho_{\max} = \min\{\rho_{sh}, V\tau\}, \quad (2.16)$$

where the shielding radius is equal to $\rho_{sh} = \frac{\Delta_e}{\omega_p}$, when $V < \Delta_e$ and $\rho_{sh} = \frac{V}{\omega_p}$, when $V > \Delta_e$. Here

Δ_e is the total electron velocity spread:

$$\Delta_e = \sqrt{\Delta_x^2 + \Delta_y^2 + \Delta_{\parallel}^2}, \quad (2.17)$$

and the plasma frequency is:

$$\omega_p = \sqrt{\frac{4\pi n_e e^2}{m}}. \quad (2.18)$$

In the case, when undulator is enable the minimum impact parameter is calculated as:

$$\rho_{\min} = \max\left(\rho_{\min}, \frac{eB\lambda^2}{4\pi^2 pc}\right), \quad (2.19)$$

where B is the undulator field, λ - its wavelength.

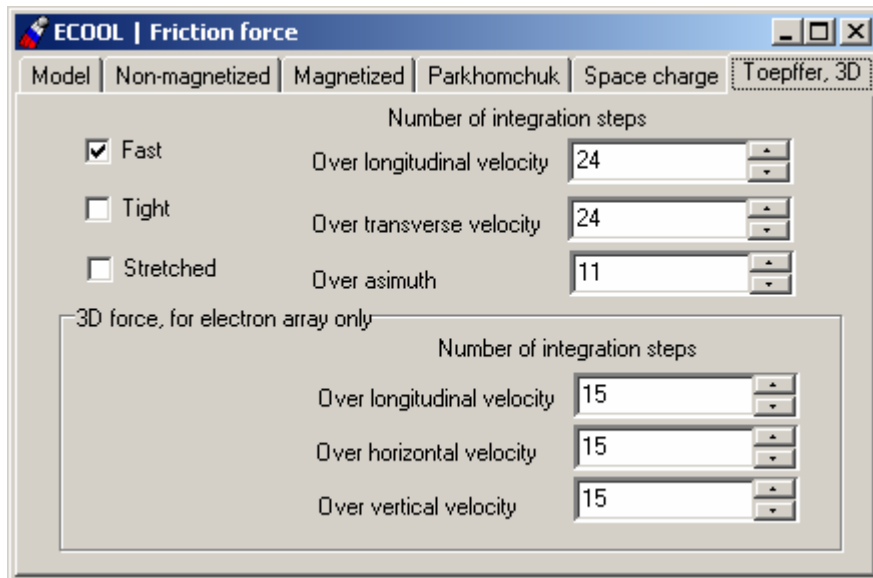


Fig. 2.1. Visual form for input parameters of Toepffer and 3D friction force calculation.

The 3D model of the friction force can be used correctly only in the case, when electron beam is presented as an array of particles. Number of integration steps over each velocity component can be input in corresponding edit windows Fig. 2.1. All the procedures for the friction force visualization can be used for 3D force also, but they output instead of transverse component of axial symmetry force the horizontal component of 3D force. The friction force is calculated in the center of the electron bunch.

2.3. Electron beam as an array of particles

To explain the structure of PARMELA output file, two first string from it are presented below:

```
20000, 3282.876465, 2.787979e+04, 5.425276e+01
-5.100488e-06 1.419776e-08 4.333701e-05 7.665530e-08 0.000000e+00 5.425276e+01 1.000000e+00
```

The first number in the first string is the particle number in the file. Last number in the first string is the mean electron kinetic energy $\langle E \rangle$ in MeV. All other strings contain parameters of individual electrons. The first four numbers are x_i, x'_i, y_i, y'_i . The fifth number is the phase φ_i in degrees relatively to RF voltage. The sixth number is the electron kinetic energy E_i in MeV. And the last number is the electron number in the array i .

In the original PARMELA file the numbers in the first string are divided by one space bar symbol. To read the file by BETACOOOL program one needs (using any text editor) to introduce symbol a few space bar or “;” between the numbers in the first string.

BETACOOOL reads the data from the file, when the radio button “From file – Gaussian” is in the position “from file”. The input file name should be introduced in the edit window of TBrowse component at the visual form (Fig. 2.2).

After reading the file BETACOOOL program calculates mean value for each co-ordinate and redefines all the electron co-ordinates in accordance:

$$x_i = x_i - \langle x \rangle. \quad (2.20)$$

Then the longitudinal electron coordinate is calculated as:

$$(s - s_0)_i = \lambda \frac{\varphi_i}{360}, \quad (2.21)$$

where $\lambda = 42.63$ cm is RF wave length.

The longitudinal momentum components of the electrons are calculated as

$$\frac{\Delta p}{p_i} = E_i \frac{(\langle E \rangle + mc^2)}{\langle E \rangle (\langle E \rangle + 2mc^2)}, \quad (2.22)$$

where $mc^2 = 0.5110034$ MeV is the electron rest energy.

The bunch charge is not presented in the file and has to be input independently in the edit window “Number of electrons”. As in other models of the electron bunch the electron array can be shifted relatively to the center of the ion bunch. The offset of the transverse and longitudinal bunch

position and angular deviation of the electron bunch orbit in respect with the ion orbit are input in the visual form “ECOOL| Cooler” in the tab sheet “Ebeam shifts”.

	Horizontal	Vertical	Longitudinal
Size, m	0.00100969102	0.00100706425	0.01073388027
Angle	5.934674162E-5	5.91288841E-5	0.00027528302

Fig. 2.2. Visual form for input and output of the electron array parameters.

Thereafter the program calculates rms values of electron co-ordinates and momentum components and output them in corresponding edit windows of the visual form. The number of particles in array is an output parameter also.

The electron beam temperatures and emittance are calculated from the array as follows:

$$T_{\perp} = mc^2 \beta^2 \gamma^2 \frac{(\sigma_{x'}^2 + \sigma_{y'}^2)}{2},$$

$$T_{\parallel} = mc^2 \beta^2 \sigma_p^2, \quad (2.23)$$

$$\varepsilon_{\perp} = \sqrt{\frac{T_{\perp} \sigma_x \sigma_y}{mc^2}}.$$

The velocity spread in the electron beam is calculated as in other electron beam models:

$$\Delta_{\perp, \parallel} = \sqrt{\frac{T_{\perp, \parallel}}{m}}. \quad (2.24)$$

All the mean bunch parameters are output in the same form, which is using for input the electron beam parameters for the other electron beam models (Fig. 2.3).

The mean electron bunch parameters are output only for comparison with other models of the electron beam, for the friction force calculation the program uses local parameters of the bunch calculated as functions of the ion co-ordinates.

The essence of the local parameter calculation is illustrated by the Fig. 2.4. In the electron array the program find N_{loc} electrons having minimum distance to the ion position. The value of N_{loc} is input in the edit window “Number of nearest particles” (Fig. 2.2). For obtained array of N_{loc}

electrons the program calculates mean and root men square parameters for all the co-ordinates and velocity components.

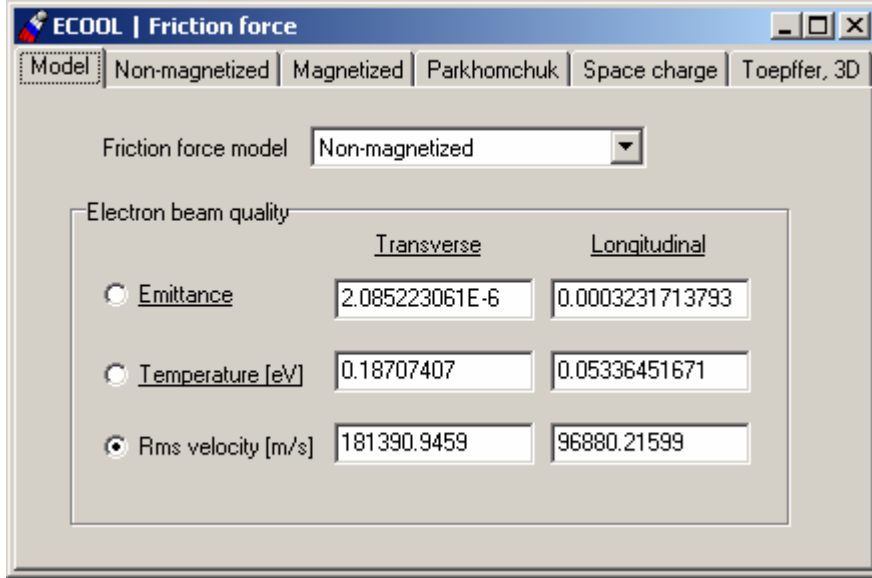


Fig. 2.3. Emittance, temperature and velocity spread of the electron array

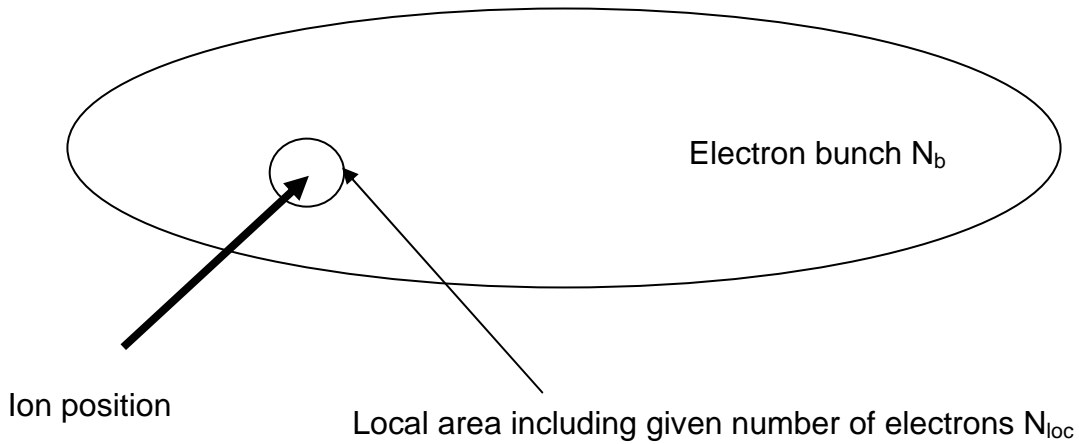


Fig.2.4. Calculation of the local electron parameters.

The algorithm of the friction force calculation is based on assumption that the local electrons are distributed in the geometry space almost uniformly. The local density is calculated via local rms values of the co-ordinates as:

$$n_e = \frac{N_e}{2\sqrt{2}2\pi\sqrt{2\pi}\sigma_x\sigma_y\sigma_s} \frac{N_{loc}}{N_{array}}, \quad (2.25)$$

where N_e is the total electron number in the bunch, N_{array} is the particle number in the file. The term $2\sqrt{2}$ in the denominator is introduced to recalculate the density for uniform distribution because at uniform distribution the beam radius is larger than its rms dimension by factor $\sqrt{2}$.

The density (2.25) and the velocity spreads (2.24) evaluated for the local array can be used for the friction force calculation in accordance with the analytical formulae (1.19) or asymptotic representation of the friction force at flattened velocity distribution. Usage of these formulae sufficiently speeds up the simulations but does not take into account asymmetry of the distribution

function in the transverse plane. If the asymmetry is sufficient one can use formulae (2.14) for 3D friction force. For this goal the corresponding electron rms velocity spreads are calculated as:

$$\Delta_{x,y} = c\beta\gamma\sigma_{x',y'}, \quad (2.26)$$

where $\sigma_{x',y'}$ are the rms angular spreads of the local electrons.

Another possibility is to calculate the friction force using velocity components of the local electrons directly. For this aim the velocities of the local electrons are recalculated into the Particle Rest Frame. The distribution function of the local electrons in the velocity space is given as a series of δ - functions:

$$f(\mathbf{v}) = \frac{1}{N_{loc}} \sum_{j=1}^{N_{loc}} \delta(\mathbf{v} - \mathbf{v}_j). \quad (2.27)$$

In the friction force formula (1.1) the integral over the distribution function is transformed into series also. In this case the friction force components are calculated as follows:

$$F_\alpha = \frac{4\pi m_e Z^2 e^4}{m} \frac{1}{N_{loc}} \sum_{j=1}^{N_{loc}} \frac{(V_\alpha - v_{j,\alpha}) L_{C,j}}{\left(\sqrt{(V_x - v_{j,x})^2 + (V_y - v_{j,y})^2 + (V_z - v_{j,z})^2} \right)^3}, \quad (2.28)$$

where V_α are the components of ion velocity in the particle rest frame, $v_{j,\alpha}$ – the velocity components of j -th electron ($\alpha = x, y, z$). The minimum impact parameter in the Coulomb logarithm $L_{C,j}$ is calculated via velocity of j -th electron:

$$\rho_{\min,j} = \frac{Ze^2}{m} \frac{1}{|\mathbf{V} - \mathbf{v}_j|^2}. \quad (2.29)$$

There is a possibility to compare the cooling process dynamics at real and Gaussian distribution of the electrons. BETACOOOL generates an array with Gaussian distribution in all degrees of freedom, when the radio button “From file – Gaussian” is in the position “Gaussian” at the visual form (Fig. 2.2). In this case the rms values of electron co-ordinates and momentum components from the corresponding edit windows of the visual form are used as input parameters, as well as the number of particles in array, which determines dimension of the created array.

2.4. Analysis of the electron distribution in array

To analyze the shape of the distribution function, when the electron bunch is presented as an array of particles, the drawing of the electron distribution can be done with BETACOOOL code in the same windows where the ion distributions are plotted during calculation process. For this one needs to push the button Open on the tab sheet Draw array of ECOOL | Electron bunch window (Fig.2.5). On the tab sheets of Beam | Real Space visual form one can see the electron distribution in different projections of six-dimensional phase space. An example of the electron distribution in array calculated with PARMELA program is presented on the Fig.2.6.

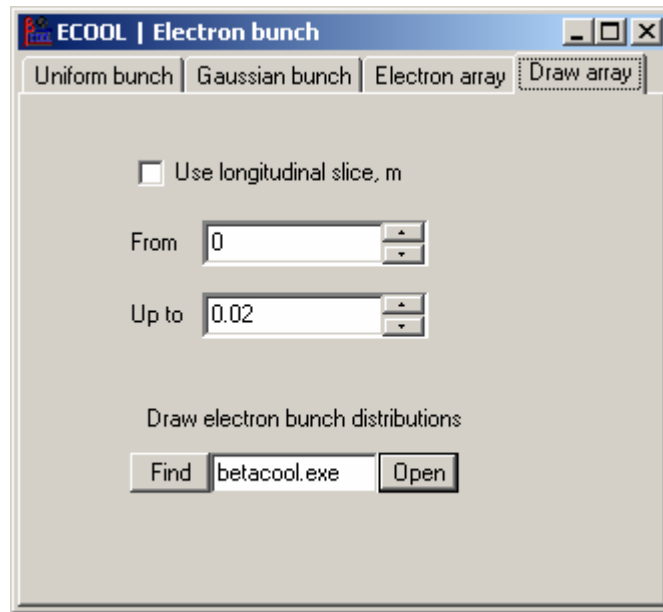


Fig.2.5. Visual form for control of output of the electron distribution in an array

On the Beam | Distribution window one can see the bunch profiles in coordinates and velocities. For bunch presented in the Fig. 2.6 the shape of profiles in transverse velocities is Gaussian practically. The profile shape in transverse co-ordinates lies between uniform and Gaussian (Fig.2.7). Peculiarities of the bunch acceleration lead to specific particle distribution in the longitudinal phase plane (right bottom plot in the Fig. 2.6.). It corresponds to well pronounced double peak structure of the beam profile in longitudinal velocity (right plot in the Fig. 2.7).

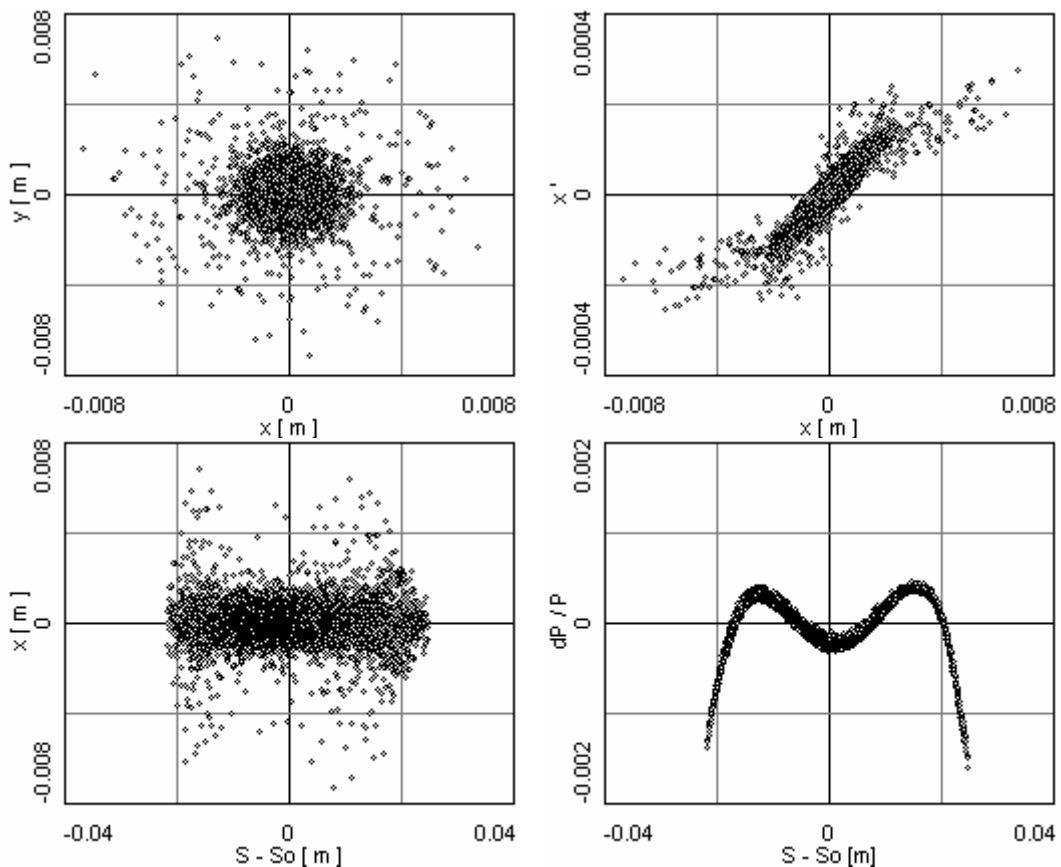


Fig.2.6. Electron distribution in the different projection of phase space. Electron co-ordinates are calculated with PARMELA code.

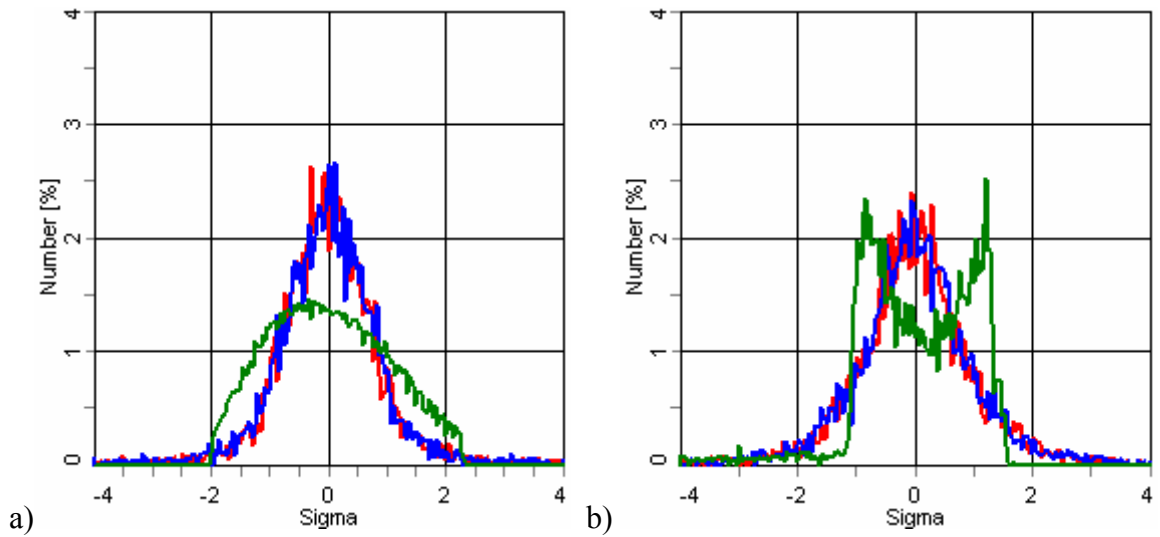


Fig.2.7. Coordinates (a) and velocities (b) distributions in the bunch shown in the Fig.2.6. Red and blue lines correspond to transverse degrees of freedom, green – longitudinal.

For such shape of longitudinal profile one can expect strong dependence of the beam emittance on the longitudinal co-ordinate in the bunch. To analyze local bunch parameters the program can output coordinates and profiles of the electrons located inside a slice lying between longitudinal co-ordinates described in the edit windows in the visual form shown in the Fig. 2.5. For this goal on the tab sheet Draw array of ECOOL | Electron bunch window (Fig.2.5) the parameter Use longitudinal slices should be enabled and the initial and final co-ordinates of the longitudinal slices should be defined. Fig. 2.8 demonstrates electron distribution in the phase space for the longitudinal slice $s = 0 \pm 0.02$ m.

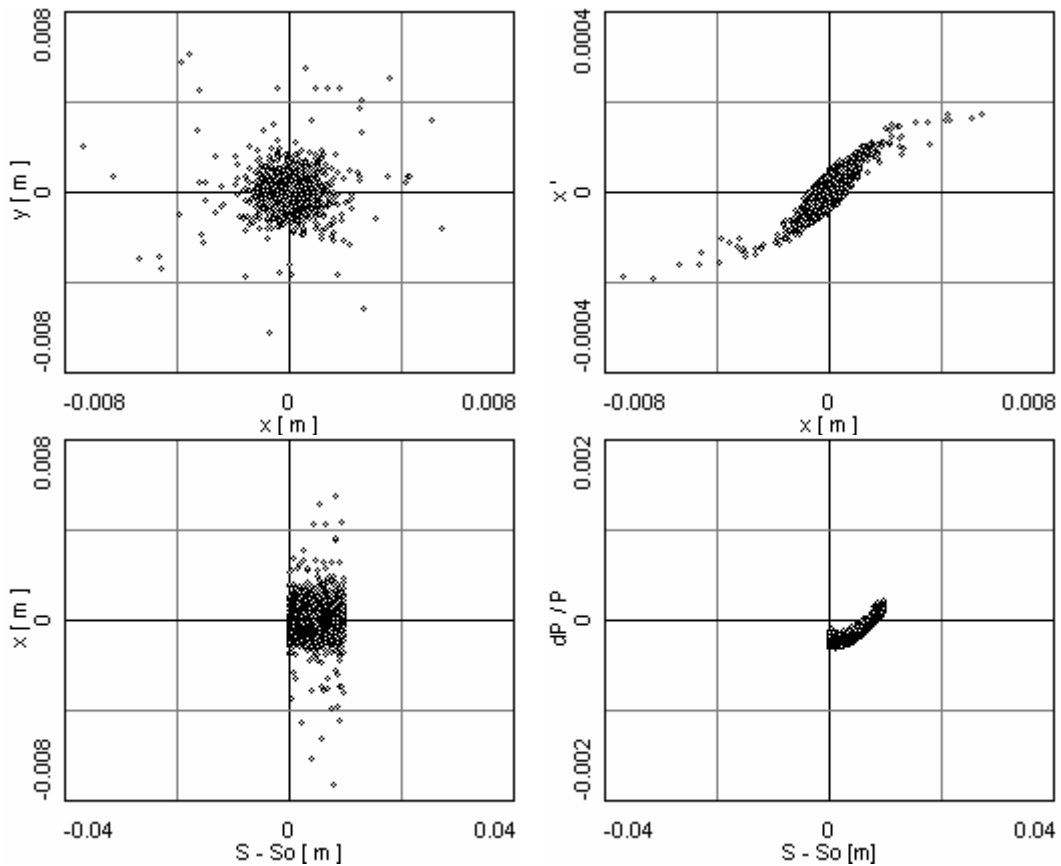


Fig.2.8. Electron distribution in the phase space for longitudinal slice $s = 0 \pm 0.02$ m.

The square of the beam cross-section (upper left plot in the Fig. 2.8) and alpha – parameter of the phase ellipse (upper right plot in the Fig. 2.8) are slightly vary from slice to slice, but the transverse profiles look like Gaussian in each longitudinal slice (Fig.2.9). The longitudinal distribution varies significantly and it is fare from Gaussian in all slices.

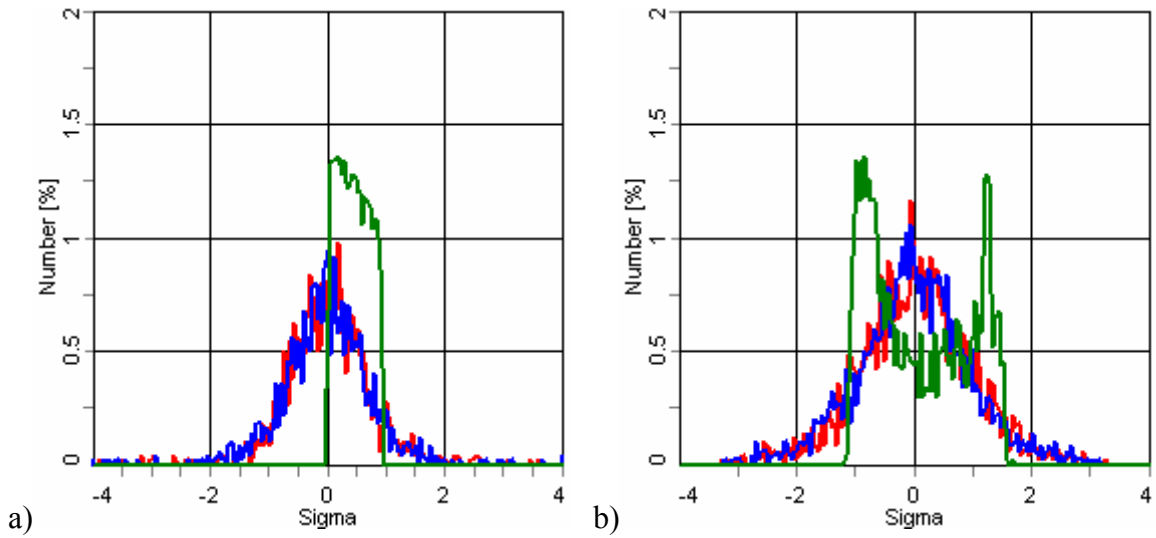


Fig.2.9. Coordinates (a) and velocities (b) distributions for longitudinal slice $s = 0 \div 2$ cm. Red and blue curves correspond to transverse degrees of freedom, green – longitudinal.

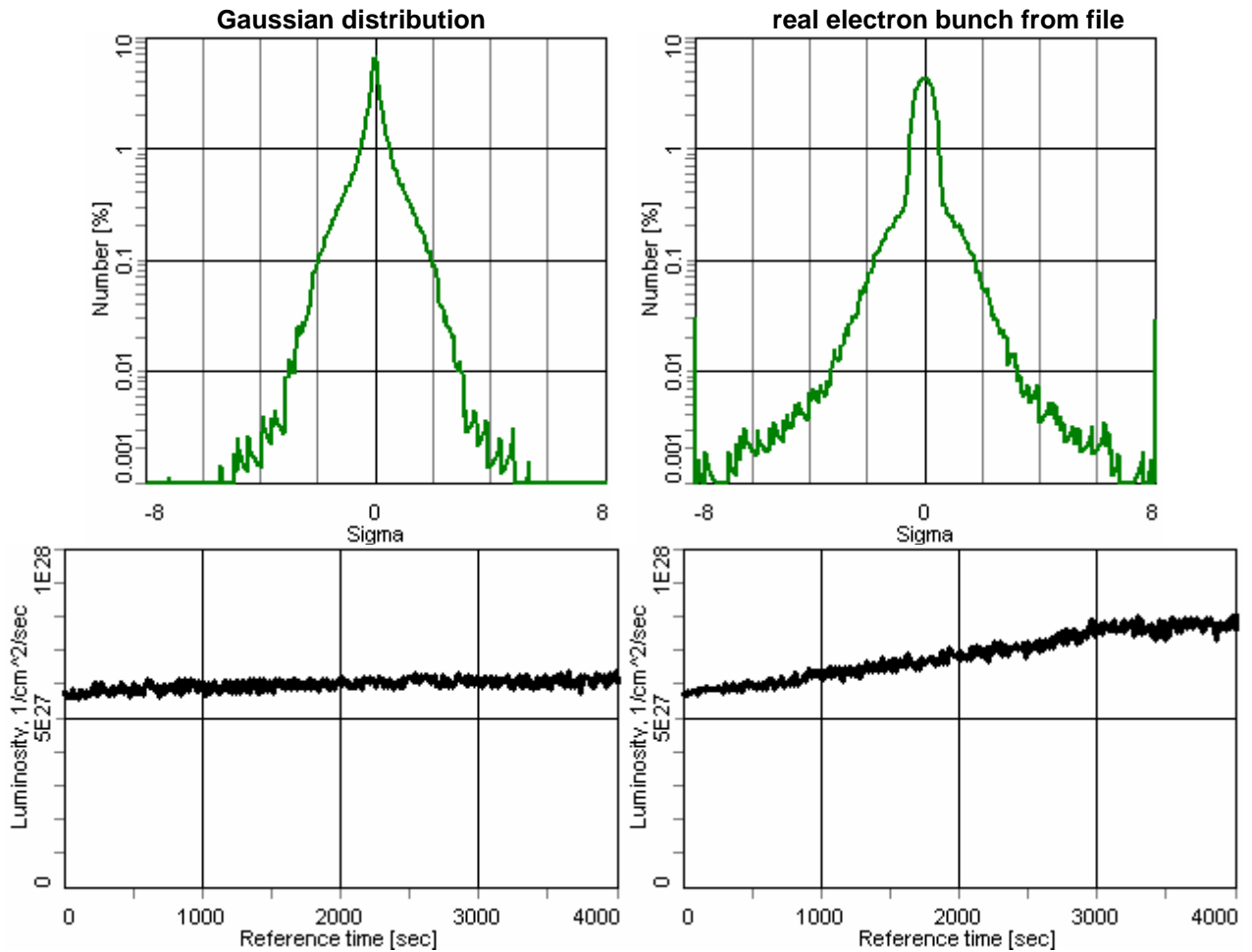


Fig.2.10. Longitudinal ion beam profile after 4000 sec of cooling process and luminosity evolution during cooling process (without intrabeam scattering) for Gaussian and real distributions of electron bunch.

The cooling process in the case of Gaussian distributions of electrons leads to formation of compact dense core in the ion bunch (upper left plot in the Fig.2.10). In the case of electron distribution show in the Fig. 2.6 the ion density in the core has a smaller value; however the core is sufficiently wider than at Gaussian distribution (upper right plot in the Fig.2.10). As a result the luminosity is larger in the case of the real distribution of electrons. This phenomenon is very similar to formation of the beam transverse emittance using “hollow” electron beam. In the presented example the “hole” (low density in the central part) in the electron bunch is formed in the space of longitudinal velocities due to peculiarities of the electron acceleration. Analogous influence on the luminosity can be provided using the painting procedure described below.

2.5. Electron beam shifts and painting procedure

In BETACOOOL code was realized different procedures for the changing of the electron beam position in transverse and longitudinal plans, the distance between electron and ion bunches, solenoid errors and so on. Parameters for these procedures were placed on different windows and sometime duplicate each other. Now all these possibilities are placed on the same tab sheet Ebeam Shifts on ECOOL | Cooler window (Fig.2.11).

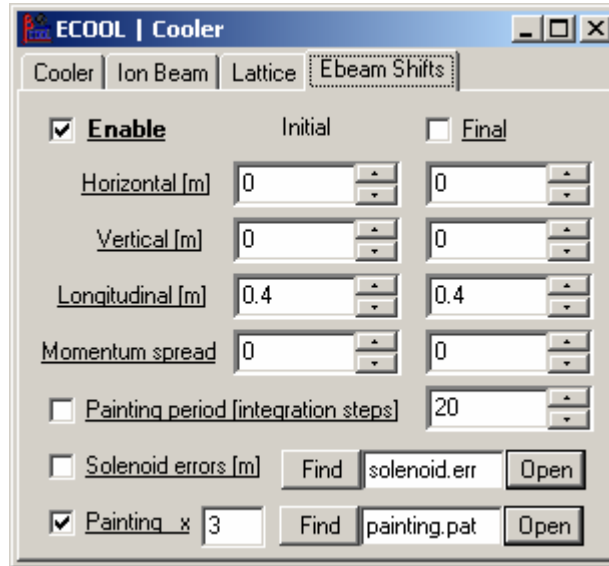


Fig.2.11. Control window for electron beam shifts and painting procedure.

The definition for the electron beam shifts in the laboratory rest frame is written as following:

$$\begin{aligned}
 \Delta x' &= (\Delta x_{fin} - \Delta x_{ini}) / l \\
 \Delta x &= \Delta x_{ini} + \Delta x' h \\
 \Delta y' &= (\Delta y_{fin} - \Delta y_{ini}) / l \\
 \Delta y &= \Delta y_{ini} + \Delta y' h \\
 \Delta(dp/p) &= \Delta(dp/p)_{ini} \\
 \Delta s &= \Delta s_{ini}
 \end{aligned}
 \tag{2.30}$$

where $(\Delta x, \Delta x', \Delta y, \Delta y', \Delta s, \Delta(dp/p))$ - vector of current shifts, $(\Delta x_{ini}, \Delta x'_{ini}, \Delta y_{ini}, \Delta y'_{ini}, \Delta s_{ini}, \Delta(dp/p)_{ini})$ and $(\Delta x_{fin}, \Delta x'_{fin}, \Delta y_{fin}, \Delta y'_{fin}, \Delta s_{fin}, \Delta(dp/p)_{fin})$ - vectors of initial and final shifts, l – distance between points of shift, h – current position of ion. If Solenoid error option is not enabled then $l = L_{ecool}$ and $h = L_{ecool} / 2$, L_{ecool} – electron cooler

length. If **Solenoid errors** option is enabled then l is the length of magnetic field inhomogeneity which calculated from input data file *.err with field errors, h is equal to difference between ion longitudinal coordinate and position of the correspondence field inhomogeneity. This file has 3 columns which correspond to the longitudinal coordinate, horizontal and vertical shifts along the longitudinal axis. Note that the **Solenoid errors** option will work properly if Euler or Runge-Kutta cooler model is chosen on the tab sheet **Cooler**.

If parameter **Final** is not enabled then final vector of shifts is equal to initial vector. The painting procedure is used when the parameter **Painting period** is enabled:

$$(\Delta x, \Delta x', \Delta y, \Delta y', \Delta s, \Delta(dp/p)) = (\Delta x, \Delta x', \Delta y, \Delta y', \Delta s, \Delta(dp/p)) \times R, \quad (2.31)$$

where R is the remainder of integer division N_{step}/P_{step} , N_{step} – step number of beam simulation, P_{step} – parameter of **Painting period**. If **Final** parameters is enabled for painting procedure then longitudinal coordinate and momentum spread shifts are calculated as

$$\begin{aligned} \Delta(dp/p) &= \Delta(dp/p)_{ini} + [\Delta(dp/p)_{fin} - \Delta(dp/p)_{ini}] \times R \\ \Delta s &= \Delta s_{ini} + (\Delta s_{fin} - \Delta s_{ini}) \times R \end{aligned} \quad (2.32)$$

Electron beam shifts can be read from the file for the painting procedure if parameters **Painting** is enabled. This file includes 6 columns which correspond to vector of current shifts. Number of rows equal to the period of the painting procedure and each row corresponds to the current step of the integration process. Scaling parameters **Painting x ___** can increase (positive value) or decrease (negative value) a speed of the painting procedure. For example, if scaling parameters equal 2 it means that only each second row is used in the painting procedure. If scaling parameter equal -2 it means that each row is used twice. User can change all parameters on the tab sheet **Ebeam Shifts** during simulation and even change data filenames with solenoid errors or painting procedure.

Example of beam dynamics without and with painting procedure for standard parameters of RHIC is presented on Fig.2.12. The electron bunch has smaller length than ion, 1 cm and 18 cm of r.m.s size correspondingly. Without painting procedure the cooling process mainly exist for central particles only and particles in tails did not cool. That leads to the increasing of transverse emittances and the decreasing of the luminosity with time.

The linear painting procedure over longitudinal position of electron bunch from 0 cm to 20 cm is presented on Fig.2.12. In this case the transverse emittances don't change during cooling process and the luminosity does not decreasing with time. The dynamics of emittances has the same behavior for the painting procedure from 0 cm to 40 cm but the maximum value of the luminosity is smaller than for previous one (Fig.2.13).

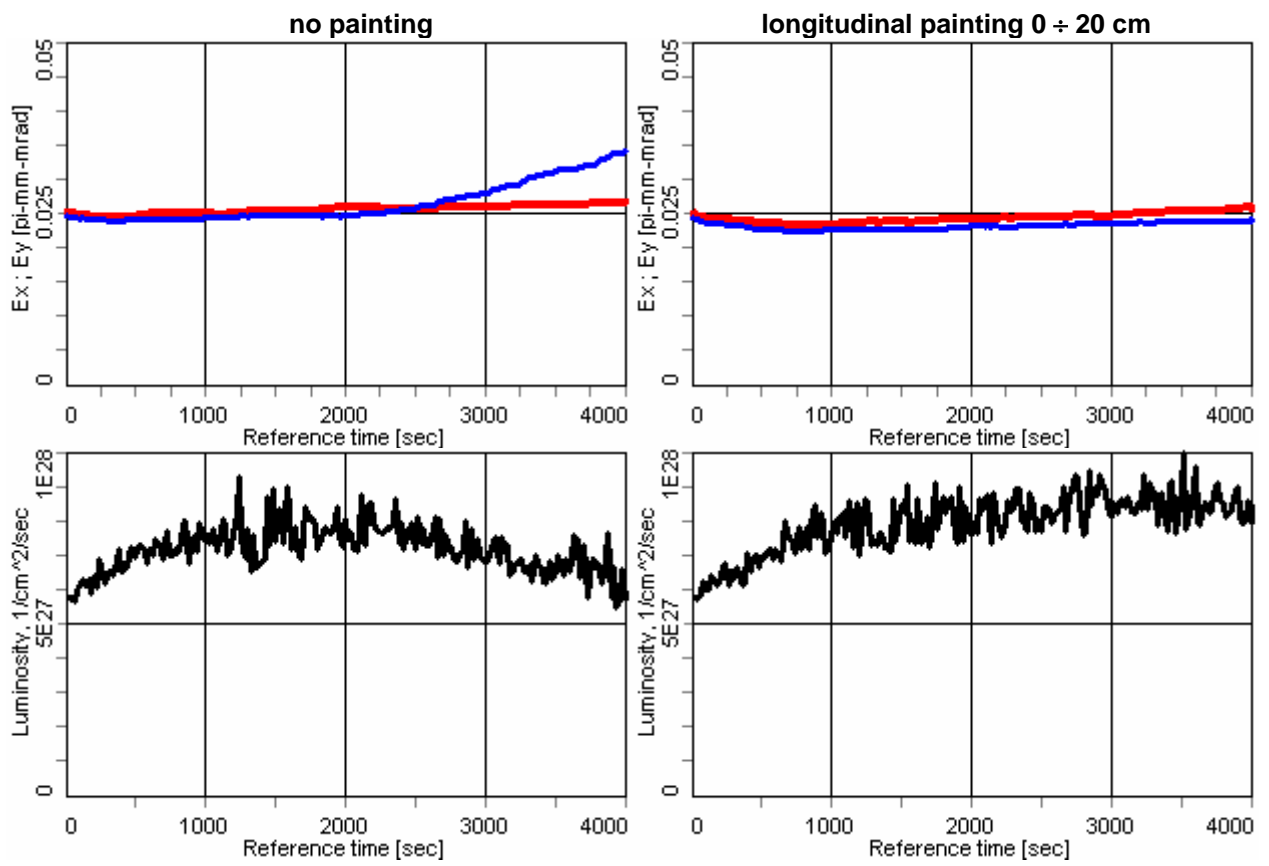


Fig.2.12. Dependence of emittances and luminosity on time without and with longitudinal painting 0÷20 cm, 200 sec total period of painting.

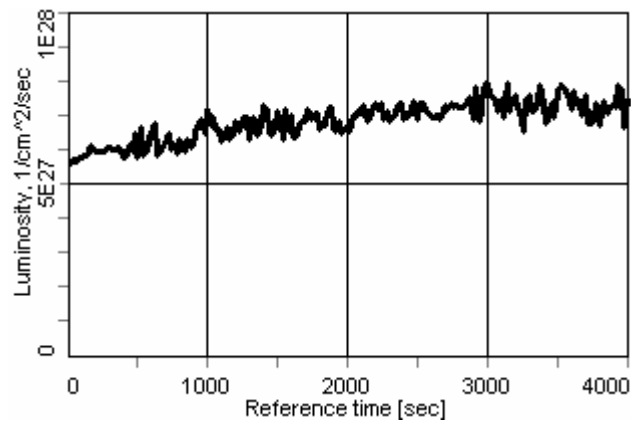


Fig.2.13. Dependence of luminosity on time with longitudinal painting 0÷40 cm.

3. STOCHASTIC COOLING SIMULATION

Algorithm for stochastic cooling simulation was implemented into BETACOOOL in accordance to the model derived by H.Stochorst (FZJ). The stochastic cooling for transverse degrees of freedom is simulated under assumption that the quarter wave loop pickup and kicker are located in the ring at positions with zero dispersion and its derivative. The phase advance of the betatron oscillations from pickup to kicker assumed to be $(2k+1)\frac{\pi}{2}$, where k is integer, and the phase errors are minimized. For two transverse degrees of freedom there is no band overlap. Cooling of longitudinal degree of freedom is simulated in accordance with the theory of filter method. The simulation presumes that the longitudinal cooling is applied using analogous system components as in the case for transverse cooling. Pickup and kicker are then operated in Σ -mode and the signal pass contains a notch filter that provides the necessary information on the energy deviation of a particle for the coherent signal. Simultaneously the filter rejects the noise signals at frequency near the revolution harmonics.

The model permits to estimate characteristic cooling times, consumption power and generate a kick of the particle momentum in the Model Beam algorithm using geometry parameters of pickup and kicker electrodes

3.1. Cooling rate calculation

The transverse emittance derivative over time in each plane can be written in the following form:

$$\frac{d\varepsilon}{dt} = -\frac{1}{\tau_{cool}}(\varepsilon - \varepsilon_{\infty}), \quad (3.1)$$

where τ_{cool} describes the drift term in the Fokker-Plank equation and the equilibrium emittance ε_{∞} corresponds to the diffusion term [3, 4]. The characteristic time of the emittance variation due to action of the stochastic cooling is equal:

$$\frac{1}{\tau} = \frac{1}{\varepsilon} \frac{d\varepsilon}{dt} = -\frac{1}{\tau_{cool}} \frac{\varepsilon - \varepsilon_{\infty}}{\varepsilon}. \quad (3.2)$$

The transverse cooling time is determined from the parameters of the cooling system as follows:

$$\frac{1}{\tau_{cool}} = \frac{16}{3} \frac{|\eta| \delta W^2}{N f_0} \cdot x J(x). \quad (3.3)$$

Here $\eta = \frac{1}{\gamma^2} - \frac{1}{\gamma_{tr}^2}$ is off-momentum factor of the storage ring, γ is Lorenz factor of the ion, γ_{tr} is critical energy of the ring in the rest energy units. f_0 is the ion revolution frequency. $W = f_{max} - f_{min}$ is the bandwidth of the system with lower frequency f_{min} and upper frequency f_{max} . N is the ion number. Total momentum spread of the beam δ is calculated from r.m.s. value in accordance with the shape of distribution function. For instance, at a parabolic distribution

$$\delta = 4 \frac{\Delta p}{p_{rms}}. \quad (3.4)$$

Formfactor $xJ(x)$ is calculated through a frequency range as follows:

$$xJ(x) = x \left(1 - 2x \ln \left(\frac{x + f_{\max}/W}{x + f_{\min}/W} \right) + \frac{x^2}{(x + f_{\max}/W)(x + f_{\min}/W)} \right). \quad (3.5)$$

The x value is proportional to the linear gain of the system from pickup to kicker G_A :

$$x = G_A / R, \quad (3.6)$$

where the coefficient R is determined by parameters of pickup and kicker:

$$R = \frac{16}{3A_2} \frac{|\eta|\delta W}{N} \frac{1}{Z} \frac{h_p h_k}{\sigma_p \sigma_k} \frac{1}{\sqrt{\beta_p \beta_k n_p n_k}} \frac{\beta p c}{(1 + \beta) e^2 f_0^2 l_{loop}}. \quad (3.7)$$

Here $h_{p,k}$ is height of the gap at pickup and kicker, the pickup and kicker sensitivity are given by

$$\sigma_{p,k} = 2 \tanh \left(\frac{\pi w_{p,k}}{2h_{p,k}} \right), \quad (3.8)$$

where $w_{p,k}$ is the electrode width, Z – characteristic impedance, $\beta_{p,k}$ – beta functions in the pickup and kicker position, $n_{p,k}$ is the number of lambda quarter loops in pickup and kicker, l_{loop} is the loop length. βc , p and e – are the ion velocity, momentum and charge correspondingly, c is the speed of light. Value A_1 is calculated through the bandwidth as follows

$$A_1 = \frac{1}{W} \int_{f_{\min}}^{f_{\max}} \sin^2 \left(\frac{2\pi f l_{loop}}{\beta c} \right) df. \quad (3.9)$$

The equilibrium emittance value is determined by the cooling system parameters and the thermal noise power:

$$\varepsilon_{\infty} = \frac{1}{4} \frac{A_3}{A_2} \sqrt{\frac{\beta_k n_k}{\beta_p n_p}} (T_A + T_R) \frac{h_p \sigma_k}{h_k \sigma_p} l_{loop} \frac{1 + \beta}{\beta p c} G_A, \quad (3.10)$$

where T_A and T_R are the pickup and preamplifier temperatures correspondingly. The values A_2 and A_3 are the following integrals:

$$A_2 = \frac{1}{W} \int_{f_{\min}}^{f_{\max}} \frac{\sin^2(2\pi f l_{loop} / \beta c)}{2\pi f l_{loop} / \beta c} df, \quad (3.11)$$

$$A_3 = \frac{1}{W} \int_{f_{\min}}^{f_{\max}} \left(\frac{\sin(2\pi f l_{loop} / \beta c)}{2\pi f l_{loop} / \beta c} \right)^2 df. \quad (3.12)$$

For longitudinal degree of freedom the cooling time calculation is based on solution of Fokker-Plank equation. The ion distribution in the energy space is described by the function $\Psi(E)$, where E is the energy deviation from mean kinetic energy E_0 . The Fokker-Plank equation for the

distribution function $\Psi(E,t)$, which describes the particle density in the energy space, has the following form

$$\frac{\partial}{\partial t} \Psi(E,t) = -\frac{\partial}{\partial E} \left[F(E)\Psi(E,t) - D(E,t)\frac{\partial}{\partial E} \Psi(E,t) \right],$$

where E is energy deviation from the mean kinetic energy E_0 .

Drift term in this equation describes the coherent cooling

$$F(E) = \frac{E}{\tau_0},$$

where τ_0 is the “single particle” cooling time. The diffusion term contains two parts

$$D(E,t) = D_{th}(E,t) + D_s(E,t)$$

the beam heating due to thermal noise

$$D_{th}(E,t) = AE^2$$

and beam heating due to the finite Schottky noise density

$$D_s(E,t) = BE^2\Psi(E,t).$$

To calculate dynamics of the rms beam parameters the Fokker-Plank equation can be reduced to equation for the second moment of the distribution function which is determined by

$$\sigma_E^2 = \frac{1}{N} \int E^2 \Psi(E) dE \quad (3.13)$$

This equation has the following form [5, 4]:

$$\frac{d\sigma_E^2}{dt} = -\frac{2}{\tau_0} \sigma_E^2 + A\sigma_E^2 + \frac{3B}{N} \int E^2 \Psi^2(E,t) dE$$

Rms dynamics algorithm presumes Gaussian distribution in all degrees of freedom. In the energy space it corresponds to the density $\rho(E,t) = \frac{1}{N} \Psi(E,t)$ given by

$$\rho = \frac{1}{\sqrt{2\pi}\sigma_E} \exp\left(-\frac{(E-E_0)^2}{2\sigma_E^2}\right).$$

Thus the integral in the last term is equal to

$$\int E^2 \Psi^2 dE = N^2 \int E^2 \rho^2 dE = \frac{N^2 \sigma_E}{4\sqrt{\pi}},$$

and evolution of the second order momentum of the distribution function is described by the following equation

$$\frac{d\sigma_E^2}{dt} = -\frac{2}{\tau_{cool}}\sigma_E^2 + \frac{3B}{4\sqrt{\pi}}N\sigma_E, \quad (3.14)$$

The values A , B , τ_{cool} and τ_0 are determined from the cooling system parameters as follows:

$$\frac{1}{\tau_{cool}} = \frac{1}{\tau_0} - 3A, \quad (3.15)$$

$$A = e^2(T_R + T_A)Zn_k \left(\frac{\kappa}{E_0}\right)^2 G_A^2 \frac{W}{f_0} \left(f_C^2 + \frac{W^2}{12}\right), \quad (3.16)$$

$$B = A_1 e^4 n_k n_p Z^2 \frac{|\kappa|}{E_0} G_A^2 f_0 f_C W, \quad (3.17)$$

the ‘‘single particle’’ cooling time τ_0 is given by

$$\frac{1}{\tau_0} = 2A_1 e^2 \sqrt{n_p n_k} Z G_A W f_C \frac{\kappa}{E_0}, \quad (3.18)$$

where $\kappa = \eta \frac{\gamma}{\gamma + 1}$, $f_C = \frac{f_{\min} + f_{\max}}{2}$ is the central frequency of the band. A_1 is determined by the formula (3.9) at the loop length of the longitudinal electrodes.

Characteristic rate for the longitudinal emittance deviation (in Betacool for the longitudinal emittance such a definition $\varepsilon_{long} = \left(\frac{\Delta p}{p}\right)^2$ is used) can be calculated in accordance with

$$\frac{1}{\tau} = \frac{1}{\varepsilon_{long}} \frac{d\varepsilon_{long}}{dt} = \frac{1}{\sigma_E^2} \frac{d\sigma_E^2}{dt} = -\frac{2}{\tau} + \frac{3BN}{4\sqrt{\pi}\sigma_E}. \quad (3.19)$$

Using relation between energy and momentum deviations $\frac{\sigma_E}{E_0} = \frac{1+\gamma}{\gamma} \frac{\Delta p}{p}$ the last equation can be reduced to:

$$\frac{1}{\tau} = -\frac{2}{\tau_{cool}} + \frac{3BN\gamma}{4\sqrt{\pi}\sqrt{\varepsilon_{long}} E_0 (1+\gamma)}. \quad (3.20)$$

3.2. Power consumption

Optimization of the cooling system parameters presumes not only minimization of the equilibrium emittance and cooling time, but also keeping a consumption power in a reasonable range. The consumption power for transverse cooling chain is calculated as a sum of thermal noise power and Schottky power. The thermal noise power in the cooling bandwidth is given by:

$$P_{th} = (T_A + T_R)G_A^2W, \quad (3.21)$$

and this value has to be corrected to take into account losses in combiner P_{comb} :

$$P_{th,tot} = P_{th} \cdot 10^{P_{comb}[dB]/10} \quad (3.22)$$

The Schottky power in the cooling band is

$$P_S = A_1 N n_p \beta_p Z \left(\frac{\sigma_p}{h_p} \right)^2 e^2 f_0 \varepsilon_{rms} G_A^2 W. \quad (3.23)$$

The total power is calculated as the sum of (3.22) and (3.23) plus losses in an electronic chain. The losses in the electronic chain are input into program as additional parameter P_{loss} and total consumption power is calculated in accordance with:

$$P_{tot} = (P_{th,tot} + P_S) \cdot 10^{P_{loss}[dB]/10}. \quad (3.24)$$

The loss power includes losses in splitter, reserve noise signal and others losses and by the order of magnitude is about 10 dB.

The filtered thermal noise power in the cooling bandwidth at the kicker input can be estimated from:

$$P_{th} = \frac{1}{3}(T_A + T_R)G_A^2W. \quad (3.25)$$

The filtered Schottky power at the kicker input is

$$P_S = 4A_1 N n_p Z e^2 G_A^2 \eta^2 \left(\frac{\Delta p}{p} \right)_{rms}^2 \frac{W}{f_0} \left(f_C^2 + \frac{W^2}{12} \right). \quad (3.26)$$

The total power consumption is calculated by the same way as for transverse degrees of freedom.

3.3. Kick of the ion momentum components due to action of stochastic cooling

In the frame of Model Beam algorithm each particle is presented as a 6 co-ordinate vector:

$\vec{X} = \left(x, \frac{p_x}{p}, y, \frac{p_y}{p}, s - s_0, \frac{\Delta p}{p} \right)$, where x and y are the horizontal and vertical co-ordinates, p_x and p_y

are corresponding momentum components, $s - s_0$ is the distance from the bunch center (in the case of coasting beam this variable can have arbitrary value), Δp is the particle momentum deviation from momentum of reference particle p .

Some effects like electron cooling or internal target are located in some fixed points of the ring. Such effects are characterizing by the ring lattice functions in the effect position. Some effects like intrabeam scattering or scattering on residual gas are distributed over the total ring circumference. Average action of such effects can be applied to the beam in ‘‘averaged’’ position in the ring, that has the beta and dispersion functions equal to averaged over the ring ones, the alpha-functions and

dispersion derivative are equal to zero. Between the effect position the particle co-ordinates are transformed using linear matrix at random phase advance (the random generation of the phase advance reflects that the integration step over time is sufficiently longer than revolution period and than betatron oscillation period). Action of each effect is simulated as the particle momentum variation in accordance with Langevin equation:

$$\left(p_{x,y,s} / p\right)_{fin} = \left(p_{x,y,s} / p\right)_{in} + \Lambda_{x,y,s} \Delta T + \sqrt{D_{x,y,s} \Delta T} \xi_{x,y,s}, \quad (3.27)$$

where p_s is the particle longitudinal momentum deviation, subscript *in* correspond to initial momentum value, subscript *fin* relates to final particle momentum after action of the effect, Λ and D are the drift and diffusion terms for corresponding degree of freedom, ΔT is step of the integration over time, ξ is Gaussian random number at unit dispersion. The regular variation of the particle momentum due to action of drift term can be rewritten as

$$\left(p_{x,y,s} / p\right)_{fin} = \left(p_{x,y,s} / p\right)_{in} \left(1 + \frac{\Lambda_{x,y,s}}{\left(p_{x,y,s} / p\right)_{in}} \Delta T\right). \quad (3.28)$$

Here the value $\frac{\Lambda_{x,y,s}}{\left(p_{x,y,s} / p\right)_{in}}$ does not depend on the effect position in the ring, and it can be treated as a “single-particle” cooling time. At large value of ΔT the absolute value of the term $\frac{\Lambda_{x,y,s}}{\left(p_{x,y,s} / p\right)_{in}} \Delta T$ can be larger than unity (in the case of cooling this term has a negative sign). In

this case direct application of the formula (3.28) will lead to change a sign of corresponding momentum component and can lead also to increase of its absolute value. This situation corresponds to artificial diffusion heating of the beam on numerical algorithm. To avoid this

“numerical” diffusion at $\left| \frac{\Lambda_{x,y,s}}{\left(p_{x,y,s} / p\right)_{in}} \Delta T \right| > 1$ the formula (3.28) is transformed to the following form

$$\left(p_{x,y,s} / p\right)_{fin} = \left(p_{x,y,s} / p\right)_{in} \times \exp\left\{\frac{\Lambda_{x,y,s}}{\left(p_{x,y,s} / p\right)_{in}} \Delta T\right\}, \quad (3.29)$$

which includes the (3.28) as a limit case at small ΔT .

In the case of random variation of the particle momentum components corresponding to diffusion term in (3.27) the kick has to be calculated taking into account the ring lattice parameters in the effect position. In the simplest case at the constant diffusion the equation for the emittance variation in time can be written as follows:

$$\frac{d\varepsilon_{x,y}}{dt} = \frac{D_{x,y}}{2\varepsilon_{x,y}}, \quad (3.30)$$

that gives

$$\Delta\varepsilon_{x,y} = \frac{D_{x,y}}{2\varepsilon_{x,y}} \Delta T. \quad (3.31)$$

Tacking into account that rms momentum variation relates to the emittance variation as $\langle \theta^2 \rangle = 2 \frac{\Delta \varepsilon_{x,y}}{\beta_{x,y}}$, for the momentum components variation we have:

$$\Delta(p_{x,y} / p) = \sqrt{\frac{D_{x,y}}{\varepsilon_{x,y} \beta_{x,y}} \Delta T \xi_{x,y}}, \quad (3.32)$$

where $\beta_{x,y}$ are the beta functions in the effect position in corresponding planes. For longitudinal degree of freedom emittance is determined as square of the rms momentum spread and at this definition we have:

$$\Delta(\Delta p / p) = \sqrt{k \frac{D_{long}}{2\varepsilon_{long}} \Delta T \xi}, \quad (3.33)$$

where $k = 1$ for coasting beam and $k = 2$ for bunched one.

For the transverse degree of freedom the drift term in (3.27) is calculated in accordance with the formula (2.3) for the ‘‘single particle’’ cooling time. The regular variation of transverse momentum component are calculated in accordance with (3.28, 3.1.29):

$$(p_{x,y} / p)_{fin} = \begin{cases} (p_{x,y} / p)_{in} \left(1 - \frac{\Delta T}{\tau_{cool,x,y}} \right), & \text{if } \left| \frac{\Delta T}{\tau_{cool,x,y}} \right| < 1 \\ (p_{x,y} / p)_{in} \exp\left(-\frac{\Delta T}{\tau_{cool,x,y}} \right), & \text{if } \left| \frac{\Delta T}{\tau_{cool,x,y}} \right| > 1 \end{cases} \quad (3.34)$$

Diffusion coefficient for the transverse degrees of freedom can be calculated using formula (3.10) for equilibrium emittance value. The emittance variation in time can be described by the following differential equation:

$$\frac{d\varepsilon_{x,y}}{dt} = -\frac{\varepsilon_{x,y}}{\tau_{cool,x,y}} + \frac{D_{x,y}}{2\varepsilon_{x,y}}. \quad (3.35)$$

From the other hand (3.1) gives

$$\frac{d\varepsilon_{x,y}}{dt} = -\frac{\varepsilon_{x,y}}{\tau_{cool,x,y}} + \frac{\varepsilon_{\infty,x,y}}{\tau_{cool,x,y}},$$

and for the diffusion coefficient we have:

$$D_{x,y} = \frac{2\varepsilon_{x,y} \varepsilon_{\infty,x,y}}{\tau_{cool,x,y}}. \quad (3.36)$$

The diffusion power is proportional to square of the linear gain G_A that can be seen from definitions of the cooling time and equilibrium emittance (3.3, 3.10). This result can be obtained

directly from expression for emittance derivative before introduction of ε_∞ as it done for instance in [3].

In accordance with (3.32) for the momentum components variation we have:

$$\Delta(p_{x,y} / p) = \sqrt{\frac{2\varepsilon_{\infty,x,y}}{\tau_{cool,x,y}\beta_{x,y}} \Delta T \xi_{x,y}}. \quad (3.37)$$

In the present version of the program the kick is applied to the ion momentum in “averaged” position of the ring.

For longitudinal degree of freedom the “single particle” cooling time τ_0 is given by (3.18), and the regular particle momentum variation is calculated as follows:

$$(\Delta p / p)_{fin} = \begin{cases} (\Delta p / p)_{in} \left(1 - k \frac{\Delta T}{\tau_0}\right), & \text{if } \left|\frac{\Delta T}{\tau_0}\right| < 1 \\ (\Delta p / p)_{in} \exp\left(-k \frac{\Delta T}{\tau_0}\right), & \text{if } \left|\frac{\Delta T}{\tau_0}\right| > 1 \end{cases} \quad (3.38)$$

At arbitrary distribution function the integral $\int E^2 \rho^2 dE$ can be estimated by the value $\frac{N^2 \sigma_E}{6}$, which is averaged for Gaussian and parabolic distributions. In this case the equation (3.14) can be rewritten as

$$\frac{d\sigma_E^2}{dt} = -\frac{2}{\tau_0} \sigma_E^2 + 3A\sigma_E^2 + \frac{B}{2} N\sigma_E$$

or tacking into account that $\frac{\sigma_E}{E_0} = \frac{1+\gamma}{\gamma} \frac{\Delta p}{p}$ and $\varepsilon_{long} = \left(\frac{\Delta p}{p}\right)^2$

$$\frac{d\varepsilon_{long}}{dt} = -\frac{2}{\tau_0} \varepsilon_{long} + 3A\varepsilon_{long} + \frac{BN\gamma}{2E_0(\gamma+1)} \sqrt{\varepsilon_{long}}$$

The thermal and Shottky diffusion terms are independent, correspondingly the momentum kick due to diffusion is calculated as:

$$\Delta(\Delta p / p) = \sqrt{\sqrt{\left(\frac{BN\gamma}{2E_0(\gamma+1)}\right)^2 \varepsilon_{long} + (3A\varepsilon_{long})^2} k\Delta T \xi_s}. \quad (3.39)$$

Visual forms for input and output parameters of the stochastic cooling system are presented at the Fig. 3.1 – 3.3. Structure of the input file corresponds to the structure of interface part.

Effects | Stochastic cooling

Horizontal | Vertical | Longitudinal | Common parameters

Use

Lower frequency: 4 GHz

Upper frequency: 8 GHz

Electrode length: 1.3 cm

Electronic gain: linear (31622,78) logarithm (90 dB)

Optimum linear gain: 115353,3095

Pickup		Kicker	
Electrode width	1.8 cm	Electrode width	1.8 cm
Gap height	1.8 cm	Gap height	1.8 cm
Number of loop pairs	128	Number of loop pairs	32
Beta function	75 m	Beta function	75 m
Approx. length	2,944 m	Approx. length	0,736 m
Sensitivity	0,9171523357	Sensitivity	0,9171523357

Thermal noise power: 0,008836277255 W

Schottky power: 0,07627264496 W

Equilibrium emittance: 1,054472121E-10 $\pi^m \cdot \text{rad}$

Cooling rate: 0,004647370273 s^{-1}

Total power: 0,9027720063 W

Optimum cooling rate: 0,006691806406 s^{-1}

Fig. 3.1. Visual form for input and output parameters for transverse cooling chain.

Effects | Stochastic cooling

Horizontal | Vertical | Longitudinal | Common parameters

Use

Lower frequency: 4 GHz

Upper frequency: 8 GHz

Electrode length: 1.3 cm

Electronic gain: linear (316227,8) logarithm (110 dB)

Optimum linear gain: 584848,7801

Pickup number of loop pairs	128	Approx length	2,944 m
Kicker number of loop pairs	32	Approx. length	0,736 m

Thermal noise power: 0,2945425752 W

Schottky power: 0,2285716053 W

Total power: 6,953901276 W

Cooling rate: 0,01319704914 s^{-1}

Optimum cooling rate: 0,02441774574 s^{-1}

Equilibrium momentum spread: 7,294449255E-6

Fig. 3.2. Visual form for input and output parameters for longitudinal cooling chain.

The screenshot shows a software window titled "Effects | Stochastic cooling" with a tabbed interface. The "Common parameters" tab is selected. The window contains the following input parameters:

Parameter	Value	Unit
Total width of momentum distribution	4	sigma
Pickup effective temperature	80	K
Preamplifier temperature	80	K
Characteristic impedance	50	Ohm
Losses in combiner	2	dB
Other losses	10	dB

Fig. 3.3. Visual form for input parameters for power consumption calculation.

4. OPTICAL STOCHASTIC COOLING

Optical stochastic cooling (OSC) is proposed for RHIC as stand-alone technique or to complement electron cooling [6], acting mainly on halo particles for which electron cooling approach is less efficient. OSC and its transit-time method were suggested to extend the stochastic cooling technique into the optical domain, with broad-band optical amplifier and undulator (wigglers) for coupling the optical radiation to charged-particle beam. Cooling results from a particle's interaction in the kicker undulator with its own amplifier radiation, emitted in the pickup undulator. The path of the particles between the pickup and kicker (called a bypass) can be designed such that each particle receives a correction kick from its own amplifier radiation toward equilibrium orbit and energy. The interaction of a particle with amplified radiation from other particles results in heating. It was shown in [7] that the balance between cooling and heating define the optimal power of amplifier needed to achieved the ultimate cooling rate that is limited only by the bandwidth of the cooling loop, pickup-amplifier-kicker. However, in all possible applications of OSC to heavy particles, including ^{79}Au ions in the RHIC, the power required in such system appears to be several orders of magnitude large then that feasible with modern optical amplifier. In this case, the amplifier's power limits the cooling time.

We define $X=(x,x',s,\delta)^T$ as the particle 4D coordinate vector, where x,x' are transverse coordinates and angles, s is the longitudinal coordinate, δ is the particle's relative energy offset. We identify the pickup undulator at a position A in the optics of the storage ring, and the kicker undulator at the position B . The beam transport from A to B can be written as $X_B=RX_A$. Consequently, $X_A=R^{-1}X_B$ and we define

$$R^{-1} = \begin{bmatrix} R_{11} & R_{12} & 0 & R_{16} \\ R_{21} & R_{22} & 0 & R_{26} \\ R_{51} & R_{23} & 1 & R_{56} \\ 0 & 0 & 0 & 1 \end{bmatrix} \quad (4.1)$$

The path-length difference on the trajectory from A to B written in terms of particle coordinates at a location B and taken relative to the equilibrium orbit is equal to

$$\Delta\ell = -(R_{51}x + R_{52}x' + R_{56}\delta) \quad (4.2)$$

This signal must be delayed to let the particle enter the kicker undulator ahead of the signal. Moreover, the path length for a signal including the delay in the amplifier must be chosen such that the equilibrium particle comes to the kicker undulator exactly at the crossover of the electric field with the electromagnetic wave of the signal. Then, the phase difference for a nonequilibrium particle is equal to

$$\varphi = \Delta\ell \frac{2\pi}{\lambda}, \quad (4.3)$$

where λ is wavelength of the undulator radiation. The particle energy right after the energy kick is

$$\delta = \delta + G \sin(\varphi), \quad (4.4)$$

where $G = -\Delta E / E_b$ is the gain amplifier, E_b is the beam energy. For simple calculation G is defined as

$$G = G_0 \cdot \Delta t \cdot \exp\left(-\frac{s - z_0}{2\sigma_z}\right), \quad (4.5)$$

Δt is time step of calculation, G_0 is input parameter in the unit δ/sec , z_0 and σ_z are parameters of the ion bunch.

The visual form for input the OSC parameters is presented in the Fig. 4.1.

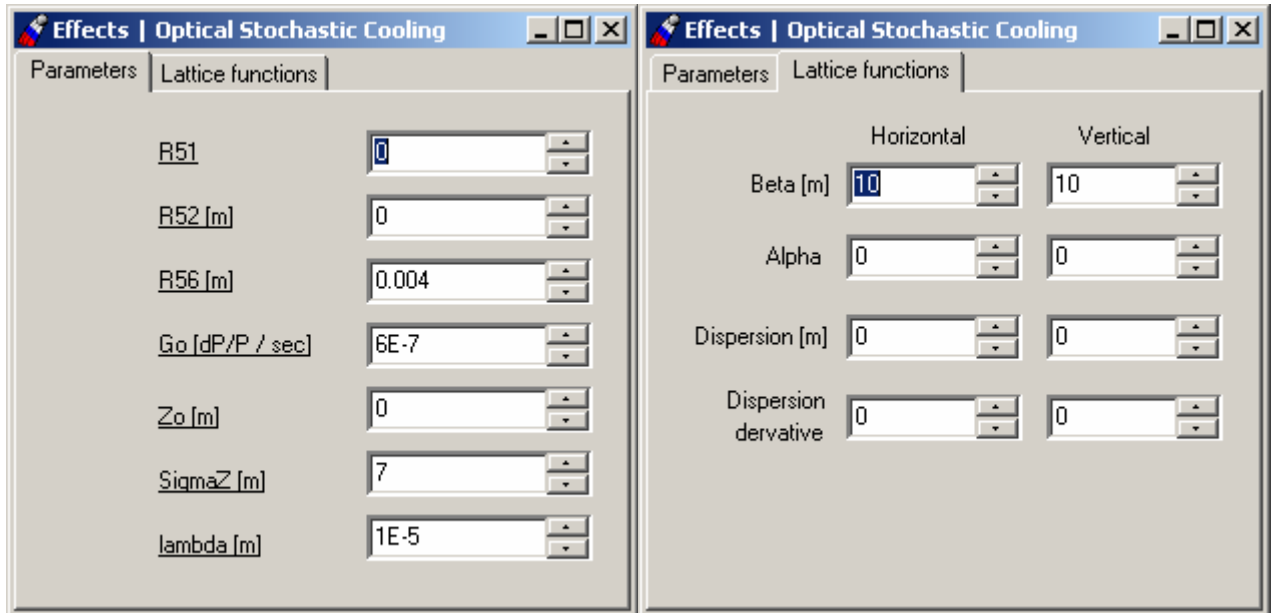


Fig.4.1. Input parameters for Optical Stochastic Cooling object.

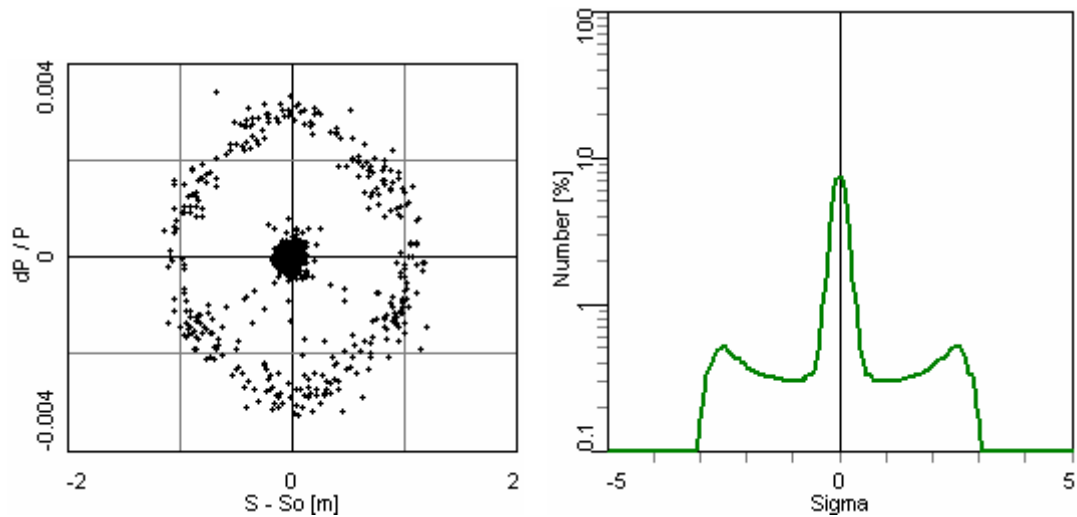


Fig. 4.2. Example of simulation using of Optical Stochastic Cooling: particle distribution in the longitudinal phase space (left) and longitudinal profile (right).

5. DEVELOPMENT OF KINETIC MODELS FOR IBS AND ECOOL

Kinetic simulation of IBS process presumes a solution of Langevin equation for each model particle. The drift and diffusion terms of the equation has to be calculated for each particle independently as a function of its co-ordinates, velocity components and distribution function of all other particles in the Model Beam.

Development of the algorithm for kinetic IBS simulation requires a solution of the following problems:

- calculation of the friction force and diffusion tensor components for a tests particle in array of field particles;
- reduction of the friction force and diffusion tensor components to the Langevin force components using to provide a kick of the particle momentum components;
- development of the algorithm structure compatible with the structure of general BETACOOOL objects.

The first task is the common for simulation of IBS and electron cooling, when the electron bunch is presented as an array of particles. In order to simplify the code benchmarking the required procedures were developed and tested for the friction and diffusion calculation in the electron bunch. The algorithm for the friction force calculation, described in the chapter 2, was modified and extended for the diffusion tensor calculation.

To benchmark the algorithm reducing friction and diffusion to Langevin force components the simplified kinetic model for IBS simulation proposed by P.Zenkevich was introduced into the code and tested. This model is based on analytical formulae for friction and diffusion components and presumes that only the friction depends on the particle velocity. The diffusion tensor in the frame of this model does not depend on the particle momentum and has a simplified structure.

In the general case all the components of the diffusion tensor have nonzero values and calculation of the Langevin force components requires analysis of the tensor eigenvalues and eigenvectors. The algorithm realizing this procedure was proposed and is under development now.

5.1. Kinetic model of IBS on the basis of Bjorken-Mtingwa theory

In the frame of Bjorken-Mtingwa model of BETACOOOL program the IBS growth rates are calculated in accordance with:

$$\left\{ \begin{array}{l} \frac{1}{\tau_x} = \left\langle \frac{H_x}{\varepsilon_x} \gamma_0^2 I_{zz} - 2 \frac{\beta_x \phi_{Bx}}{\varepsilon_x} \gamma_0 I_{xz} + \frac{\beta_x}{\varepsilon_x} I_{xx} \right\rangle_s \\ \frac{1}{\tau_y} = \left\langle \frac{H_y}{\varepsilon_y} \gamma_0^2 I_{zz} - 2 \frac{\beta_y \phi_{By}}{\varepsilon_y} \gamma_0 I_{yz} + \frac{\beta_y}{\varepsilon_y} I_{yy} \right\rangle_s \\ \frac{1}{\tau_z} = \left\langle \frac{1}{2} \frac{\gamma_0^2}{\sigma_p^2} I_{zz} \right\rangle_s \end{array} \right. , \quad (5.1)$$

where $\phi_{Bi} = D_i' + \alpha_i D_i / \beta_i$, $H_i = \beta_i D_i'^2 + 2\alpha_i D_i D_i' + \gamma D_i^2$ and $\alpha_i, \beta_i, \gamma_i$ - lattice functions in the horizontal ($i=x$) and vertical ($i=y$) plane, $\varepsilon_{x,y}$ are the horizontal and vertical emittances, σ_p – rms momentum spread. Angular brackets mean averaging over the ring circumference.

At zero vertical dispersion these formulae coincide with original Bjorken-Mtingwa theory. The collision coefficients I_{ij} are calculated in each position of the ring by numerical evaluation of the following integrals

$$I_{ij} \equiv \frac{d(P_i P_j)}{dt} = A \int_0^\infty d\lambda \frac{\lambda^{1/2}}{\sqrt{\det \Lambda}} (\delta_{ij} Tr \Lambda^{-1} - 3\Lambda_{ij}^{-1}), \quad (5.2)$$

where the matrix $A = I\lambda + L$, I – unit matrix, and matrix L is calculated via beam rms parameters and ring lattice functions in accordance with:

$$L = \begin{bmatrix} \frac{\beta_x}{\varepsilon_x} & 0 & -\gamma_0 \frac{\beta_x \phi_{Bx}}{\varepsilon_x} \\ 0 & \frac{\beta_y}{\varepsilon_y} & -\gamma_0 \frac{\beta_y \phi_{By}}{\varepsilon_y} \\ -\gamma_0 \frac{\beta_x \phi_{Bx}}{\varepsilon_x} & -\gamma_0 \frac{\beta_y \phi_{By}}{\varepsilon_y} & \frac{\gamma_0^2 H_x}{\varepsilon_x} + \frac{\gamma_0^2 H_y}{\varepsilon_y} + \frac{\gamma_0^2}{\sigma_p^2} \end{bmatrix}, \quad (5.3)$$

The IBS constant A is determined as in other IBS models:

$$A = \frac{cr_i^2 NL_c}{8\pi\beta^3 \gamma_0^2 \varepsilon_x \varepsilon_y \sigma_p \sigma_s}. \quad (5.4)$$

Here β and γ_0 are the Lorenz parameters, r_i is the ion classical radius, N is the ion number, L_c is the Coulomb logarithm, which is introduced as an input parameter.

At ion distribution function closed to Gaussian one the kinetic simulation of IBS process in the frame of Model Beam algorithm is realized on the basis of the following simplifications:

- the components of the friction force are a linear functions of the ion momentum
 $F_i = -K_i P_i$, where K_i are the constants,
- the components of the diffusion tensor D_{ij} do not depend on the ion momentum.

The model particle momentum variation after crossing an optic element of length l_k are calculated in accordance with Langevin equation:

$$P_i(t + \Delta t) = P_i(t) - K_i P_i(t) \Delta t \frac{l_k}{C} + \sqrt{\Delta t \frac{l_k}{C}} \sum_{j=1}^3 C_{i,j} \xi_j, \quad (5.5)$$

where ξ_j are three Gaussian random numbers with unit dispersion. The coefficients $C_{i,j}$ have to be calculated from diffusion and friction coefficients. Total momentum variation is calculated in cycle over optic elements along the ring circumference C .

The diffusion tensor men components in the frame of Bjorken –Mtingwa model are calculated as the following integrals:

$$D_{i,j} = A \int_0^\infty d\lambda \frac{\lambda^{1/2}}{\sqrt{\det \Lambda}} (\delta_{ij} Tr \Lambda^{-1} - \Lambda_{ij}^{-1}). \quad (5.6)$$

The collision coefficients can be expressed via friction and diffusion components as follows:

$$\left\langle \frac{d(P_i P_j)}{dt} \right\rangle = -(K_i + K_j) \langle P_i P_j \rangle + D_{i,j}, \quad (5.7)$$

where triangular brackets mean averaging over the particles. $\delta_{i,j}$ is the Kronecker-Kapelli symbol.

Comparing (5.2) and (5.7) one can find expressions for the friction coefficients:

$$K_i = \frac{A}{\langle P_i^2 \rangle_0} \int_0^\infty d\lambda \frac{\lambda^{1/2}}{\sqrt{\det \Lambda}} \Lambda_{ii}^{-1}. \quad (5.8)$$

To find expressions for $C_{i,j}$ lets multiply the momentum variation for i and j -th particles:

$$\begin{aligned} P_i(t + \Delta t) P_j(t + \Delta t) &= \left(P_i(t) - K_i P_i(t) \Delta t + \sqrt{\Delta t} \sum_{k=1}^3 C_{i,k} \xi_k \right) \left(P_j(t) - K_j P_j(t) \Delta t + \sqrt{\Delta t} \sum_{k=1}^3 C_{j,k} \xi_k \right) = \\ &= P_i(t) P_j(t) - (K_i + K_j) P_i(t) P_j(t) \Delta t + K_i K_j P_i(t) P_j(t) (\Delta t)^2 + P_i(t) \sqrt{\Delta t} \sum_{k=1}^3 C_{j,k} \xi_k + \\ &\quad + P_j(t) \sqrt{\Delta t} \sum_{k=1}^3 C_{i,k} \xi_k + \sum_{k=1}^3 C_{i,k} \xi_k \sum_{k=1}^3 C_{j,k} \xi_k \Delta t \end{aligned}$$

and average this expression over the particles. Neglecting the term $(\Delta t)^2$ and taking into account that

$$\left\langle P_j(t) \sqrt{\Delta t} \sum_{k=1}^3 C_{i,k} \xi_k \right\rangle = 0,$$

$$\langle \xi_i \xi_j \rangle = \delta_{i,j},$$

we obtain

$$\frac{\langle \Delta P_i P_j \rangle}{\Delta t} = -(K_i + K_j) \langle P_i P_j \rangle + \sum_{k=1}^3 C_{i,k} C_{j,k}. \quad (5.9)$$

The coefficients $C_{i,k}$ have to be chosen to obtain the same values of collision integrals (5.7), that gives the following system of equations:

$$-(K_i + K_j) \langle P_i P_j \rangle + \sum_{k=1}^3 C_{i,k} C_{j,k} = -(K_i + K_j) \langle P_i P_j \rangle + D_{i,j}. \quad (5.10)$$

Due to diagonal symmetry of the diffusion tensor the system consists of the following 6 independent equations for 9 unknown coefficients:

$$C_{x,1} C_{y,1} + C_{x,2} C_{y,2} + C_{x,3} C_{y,3} = D_{x,y}$$

$$\begin{aligned}
C_{x,1}C_{z,1} + C_{x,2}C_{z,2} + C_{x,3}C_{z,3} &= D_{x,z} \\
C_{y,1}C_{z,1} + C_{y,2}C_{z,2} + C_{y,3}C_{z,3} &= D_{y,z} \\
C_{x,1}^2 + C_{x,2}^2 + C_{x,3}^2 &= D_{x,x} \\
C_{y,1}^2 + C_{y,2}^2 + C_{y,3}^2 &= D_{y,y} \\
C_{z,1}^2 + C_{z,2}^2 + C_{z,3}^2 &= D_{z,z}
\end{aligned} \tag{5.11}$$

This system has an infinite number of solutions and can be simplified, when the diffusion tensor has a zero components. In our case $D_{x,y} = 0$ and $\langle P_x P_y \rangle = 0$, the solution can be build by the following way. Lets assume, that the random number ξ_1 correspond to scattering in horizontal plane, ξ_2 – in vertical and put $C_{x,2} = C_{y,1} = 0$. From the first equation of the system (5.10) follows that $C_{x,3}C_{y,3} = 0$. Lets put $C_{x,3} = 0$. In this case

$$C_{x,1} = \sqrt{D_{x,x}}. \tag{5.12}$$

From the second equation of (5.10) follows

$$C_{z,1} = \frac{D_{x,z}}{\sqrt{D_{x,x}}}. \tag{5.13}$$

Then, for simplicity put

$$C_{y,2} = C_{y,3} = \sqrt{D_{y,y}/2}. \tag{5.14}$$

From the third equation of (5.10):

$$C_{z,2} = \frac{D_{y,z}}{\sqrt{D_{y,y}/2}} - C_{z,3}. \tag{5.15}$$

Substituting (5.13) and (5.15) into the last equation of (5.10) we obtain quadratic equation about $C_{z,3}$:

$$C_{z,3}^2 - \frac{D_{y,z}}{\sqrt{D_{y,y}/2}} C_{z,3} + \frac{(D_{x,z})^2}{2D_{x,x}} + \frac{(D_{y,z})^2}{D_{y,y}} - \frac{D_{z,z}}{2} = 0.$$

In absence of vertical dispersion ($D_{y,z} = 0$, $\langle P_y P_z \rangle = 0$) it gives

$$C_{z,3} = \sqrt{\frac{D_{z,z}}{2} - \frac{(D_{x,z})^2}{2D_{x,x}}}. \tag{5.16}$$

In the general case

$$C_{z,3} = \frac{D_{y,z}}{\sqrt{2D_{y,y}}} \pm \sqrt{\frac{D_{z,z}}{2} - \frac{(D_{x,z})^2}{2D_{x,x}} - \frac{(D_{y,z})^2}{2D_{y,y}}}. \quad (5.17)$$

Fixing the sign plus in the last expression one can write total set of the coefficients:

$$\begin{aligned} C_{x,1} &= \sqrt{D_{x,x}}, \\ C_{y,2} &= C_{y,3} = \sqrt{D_{y,y}/2}, \\ C_{z,1} &= \frac{D_{x,z}}{\sqrt{D_{x,x}}}, \\ C_{z,2} &= \frac{D_{y,z}}{\sqrt{D_{y,y}/2}} - \sqrt{\frac{DetD}{2D_{x,x}D_{y,y}}}, \\ C_{z,3} &= \frac{D_{y,z}}{\sqrt{2D_{y,y}}} + \sqrt{\frac{DetD}{2D_{x,x}D_{y,y}}}, \end{aligned} \quad (5.18)$$

all the other are equal to zero. Here $DetD$ is the determinant of the matrix

$$\begin{pmatrix} D_{x,x} & 0 & D_{x,z} \\ 0 & D_{y,y} & D_{y,z} \\ D_{x,z} & D_{y,z} & D_{z,z} \end{pmatrix}, \quad (5.19)$$

D_{ij} are calculated in accordance with (5.6).

Taking into account that the diffusion and friction components are determined for the following momentum components:

$$\left(x' - D'_x \frac{\Delta p}{p}, y' - D'_y \frac{\Delta p}{p}, \frac{1}{\gamma} \frac{\Delta p}{p} \right), \quad (5.20)$$

the variations of the ion momentum components inside k -th optic element are given by

$$\Delta x'_n = -F_x \frac{\left(x'_n - D'_x \frac{\Delta p}{p_n} \right) \beta_{x,k}}{\varepsilon_x (1 + \alpha_{x,k}^2)} \Delta t \frac{l_k}{C} + \sqrt{D_{x,x} \Delta t \frac{l_k}{C}} \xi_1, \quad (5.21)$$

$$\Delta y'_n = -F_y \frac{\left(y'_n - D'_y \frac{\Delta p}{p_n} \right) \beta_{y,k}}{\varepsilon_y (1 + \alpha_{x,k}^2)} \Delta t \frac{l_k}{C} + \sqrt{\frac{D_{y,y}}{2} \Delta t \frac{l_k}{C}} \xi_1 + \sqrt{\frac{D_{y,y}}{2} \Delta t \frac{l_k}{C}} \xi_2, \quad (5.22)$$

$$\Delta \frac{\Delta p}{p_n} = -F_z \frac{\gamma \frac{\Delta p}{p_n}}{\varepsilon_{long}} \Delta t \frac{l_k}{C} + \sqrt{\Delta t \frac{l_k}{C}} \gamma C_{z,1} \xi_1 + \sqrt{\Delta t \frac{l_k}{C}} \gamma C_{z,2} \xi_2 + \sqrt{\Delta t \frac{l_k}{C}} \gamma C_{z,3} \xi_3, \quad (5.23)$$

here n is the number of the particle, $\varepsilon_{x,y}$ – horizontal and vertical emittances, α_k, β_k, D_k' – lattice parameters, longitudinal emittance is determined as $\varepsilon_{long} = \sigma_p^2$, γ is Lorenz factor, the friction coefficients F_i are calculated in accordance with:

$$F_{x,y} = \frac{\beta_{x,y}}{\varepsilon_{x,y}(1 + \alpha_{x,y}^2)} A \int_0^\infty d\lambda \frac{\lambda^{1/2}}{\sqrt{\det \Lambda}} \Lambda_{ii}^{-1}, \quad (5.24)$$

$$F_z = \frac{1}{\varepsilon_{long}} A \int_0^\infty d\lambda \frac{\lambda^{1/2}}{\sqrt{\det \Lambda}} \Lambda_{ii}^{-1}. \quad (5.25)$$

To simulate the ion motion in the case of coupling between transverse planes, after each step of integration over time the beam is rotated by 90° around axis. For each particle its co-ordinates are changed in accordance with the following equation:

$$\begin{pmatrix} x \\ y \end{pmatrix} = \begin{pmatrix} 0 & -1 \\ 1 & 0 \end{pmatrix} \begin{pmatrix} x \\ y \end{pmatrix}_0. \quad (5.26)$$

5.2. Benchmarking of the kinetic model

For Gaussian distribution the described kinetic model has to coincide with Rms dynamics simulation using Bjorken-Mtingwa model. Comparison of the kinetic model and Rms dynamics simulations are presented in the Fig. 5.1, 5.2. The simulations were performed at typical RHIC parameters. Even at model particle number of 2000 the coincidence is satisfactory.

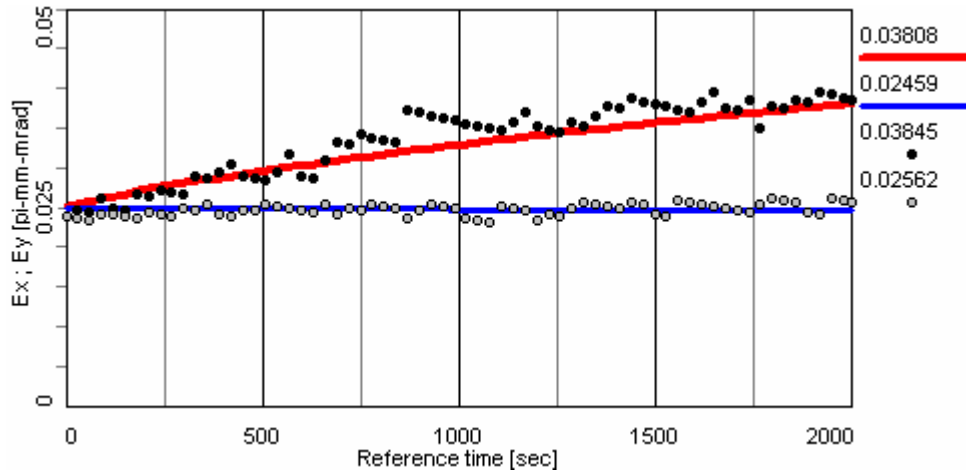


Fig. 5.1. Horizontal emittance time dependence. RMS dynamics – read solid line, kinetic model (2000 particles) – black dots. Vertical emittance time dependence. RMS dynamics – blue solid line, kinetic model (2000 particles) – gray dots.

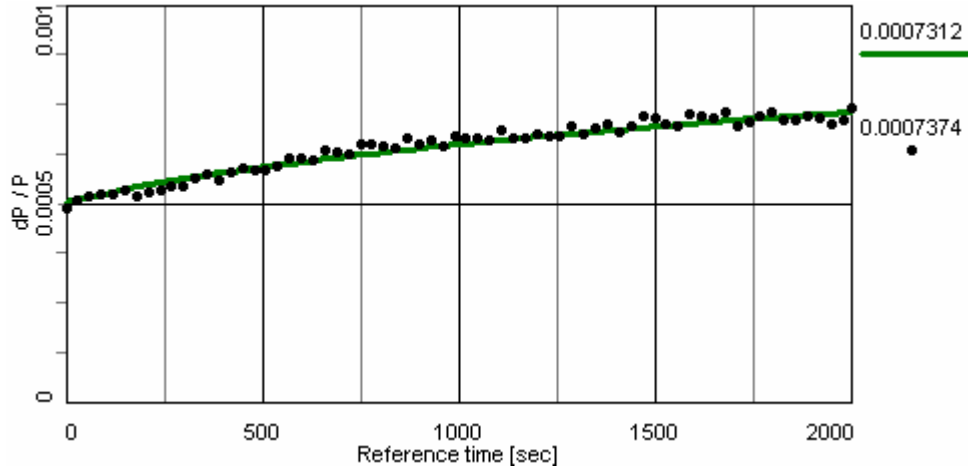


Fig. 5.2. Momentum spread time dependence. RMS dynamics solid line, kinetic model (2000 particles) – black dots.

5.3. Friction and diffusion in the array of particles

Calculation of the friction force and diffusion tensor components related with the problem of coulomb scattering of a test particle of a mass m_t and velocity of \vec{V} in an array of N_{loc} field particles of a mass m_f and velocities \vec{v}_i (Fig. 5.3).

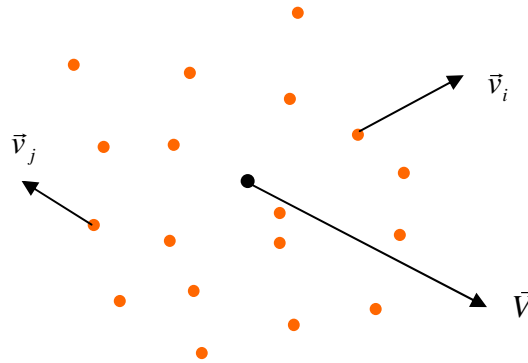


Fig. 5.3. Test particle (black circle) in the local cloud of field particles (colored circles).

Solution of this problem is well known from the plasma physics. At the distribution function of the field particles in the velocity space of $f(v)$ the friction force is equal to

$$\bar{F} = \frac{\langle \Delta \vec{p} \rangle}{\Delta t} = - \frac{4\pi m e^4 Z_t^2 Z_f^2}{\left(\frac{m_f m_t}{m_f + m_t} \right)} \int \ln \left(\frac{\rho_{\max}}{\rho_{\min}} \right) \frac{\vec{U}}{U^3} f(v) d^3 v \quad (5.27)$$

and the diffusion tensor components are

$$D_{\alpha, \beta} = \frac{\langle \Delta p_\alpha \Delta p_\beta \rangle}{\Delta t} = 4\pi m e^4 Z_t^2 Z_f^2 \int \ln \left(\frac{\rho_{\max}}{\rho_{\min}} \right) \frac{U^2 \delta_{\alpha, \beta} - U_\alpha U_\beta}{U^3} f(v) dv. \quad (5.28)$$

Here $\alpha, \beta = x, y, z$, the angular brackets mean averaging over the field particles, Z_t, Z_f are the charge numbers of the test and field particle, $\vec{U} = \vec{V} - \vec{v}$ is the relative velocity of the test and field particle. The minimum and maximum impact parameters are determined as in electron cooling simulation.

The distribution function of the field particles in the velocity space is given as a series of δ -functions:

$$f(\mathbf{v}) = \frac{1}{N_{loc}} \sum_{j=1}^{N_{loc}} \delta(\vec{v} - \vec{v}_j). \quad (5.29)$$

$$F_\alpha = \frac{4\pi n Z_t^2 Z_f^2 e^4}{\left(\frac{m_f m_t}{m_f + m_t}\right)} \frac{1}{N_{loc}} \sum_{j=1}^{N_{loc}} \frac{(V_\alpha - v_{j,\alpha}) L_{C,j}}{\left(\sqrt{(V_x - v_{j,x})^2 + (V_y - v_{j,y})^2 + (V_z - v_{j,z})^2}\right)^3} \quad (5.30)$$

n – mean local density of the field particles, N_{loc} – number of the local field particles, V_α is the component of the test particle velocity, $v_{j,\alpha}$ – velocity component of j -th field particle, $\alpha = x, y, z$. The minimum impact parameter in the Coulomb logarithm is calculated as

$$\rho_{min} = \frac{Z_t Z_f e^2}{\left(\frac{m_f m_t}{m_f + m_t}\right)} \frac{1}{|\vec{V} - \vec{v}_j|^2}. \quad (5.31)$$

The dynamic shielding radius value required for the maximum impact parameter determination is calculated using rms velocity spread of the field particles.

The components of the diffusion tensor are

$$D_{\alpha,\beta} = 4\pi n Z_t^2 Z_f^2 e^4 \frac{1}{N_{loc}} \sum_{j=1}^{N_{loc}} \frac{\left(\left((V_x - v_{j,x})^2 + (V_y - v_{j,y})^2 + (V_z - v_{j,z})^2\right) \delta_{\alpha\beta} - (V_\alpha - v_{j,\alpha})(V_\beta - v_{j,\beta})\right) L_{C,j}}{\left(\sqrt{(V_x - v_{j,x})^2 + (V_y - v_{j,y})^2 + (V_z - v_{j,z})^2}\right)^3} \quad (5.32)$$

All the values are calculated in the particle rest frame. In the general case all the components of the diffusion tensor have nonzero values.

The presented formulae can be used for electron cooling simulation, when the electron bunch is presented as an array of particles, as well as for IBS simulation in the frame of Model Beam algorithm.

An universal procedure for the friction and diffusion calculation is presently under development. It is being benchmarked for the effect ECOOL with real electron distribution represented by an array of particles.

5.4. Simulation of diffusion processes in model beam

The model particle momentum variation after crossing an optic element providing a diffusion due to some physics process (IBS, scattering on gas and so on) are calculated in accordance with Langevin equation:

$$P_i(t + \Delta t) = P_i(t) + \sqrt{\Delta t} \sum_{j=1}^3 C_{i,j} \xi_j, \quad (5.33)$$

where ξ_j are three Gaussian random numbers with unit dispersion. The coefficients $C_{i,j}$ have to be calculated from diffusion tensor coefficients.

In the general case the diffusion tensor components form a diagonal symmetric matrix:

$$\begin{pmatrix} D_{x,x} & D_{x,y} & D_{x,z} \\ D_{x,y} & D_{y,y} & D_{y,z} \\ D_{x,z} & D_{y,z} & D_{z,z} \end{pmatrix}, \quad (5.34)$$

and depending on the process some of them can be equal to zero.

In the presence of the diffusion the mean values of the momentum component variation can be expressed via diffusion tensor components in accordance with the definition:

$$\left\langle \frac{d(P_i P_j)}{dt} \right\rangle = D_{i,j}, \quad (5.35)$$

where triangular brackets mean averaging over the particles.

To find expressions for $C_{i,j}$ lets multiply the momentum variation for i and j -th particles:

$$\begin{aligned} P_i(t + \Delta t)P_j(t + \Delta t) &= \left(P_i(t) + \sqrt{\Delta t} \sum_{k=1}^3 C_{i,k} \xi_k \right) \left(P_j(t) + \sqrt{\Delta t} \sum_{k=1}^3 C_{j,k} \xi_k \right) = \\ &= P_i(t)P_j(t) + P_i(t)\sqrt{\Delta t} \sum_{k=1}^3 C_{j,k} \xi_k + \\ &+ P_j(t)\sqrt{\Delta t} \sum_{k=1}^3 C_{i,k} \xi_k + \sum_{k=1}^3 C_{i,k} \xi_k \sum_{k=1}^3 C_{j,k} \xi_k \Delta t \end{aligned}$$

and average this expression over the particles. Taking into account that

$$\left\langle P_j(t) \sqrt{\Delta t} \sum_{k=1}^3 C_{j,k} \xi_k \right\rangle = 0,$$

$$\left\langle \xi_i \xi_j \right\rangle = \delta_{i,j},$$

we obtain

$$\frac{\langle \Delta P_i P_j \rangle}{\Delta t} = \sum_{k=1}^3 C_{i,k} C_{j,k} . \quad (5.36)$$

($\delta_{i,j}$ is the Kronecker-Kapelli symbol.) The coefficients $C_{i,k}$ have to be chosen to obtain the same values of momentum variation (5.35), that gives the following system of equations:

$$\sum_{k=1}^3 C_{i,k} C_{j,k} = D_{i,j} , \quad (5.37)$$

or in the matrix form:

$$CC^T = D . \quad (5.38)$$

For instance at diagonal diffusion tensor in the case when the momentum component variations do not correlate with each other, the simplest solution is:

$$C_{x,1} = \sqrt{D_{x,x}} , C_{y,2} = \sqrt{D_{y,y}} , C_{z,3} = \sqrt{D_{z,z}} ,$$

all the other coefficients are equal to zero.

The diffusion tensor has a diagonal form in the basis formed from its eigenvectors. Lets assume that

$$\vec{Y}_i = \begin{pmatrix} Y_{i,x} \\ Y_{i,y} \\ Y_{i,z} \end{pmatrix} , i = 1, 2, 3 \quad (5.39)$$

are three linearly independent eigenvectors of the matrix D corresponding to eigenvalues λ_i . In the basis of vectors $\vec{Y}_1, \vec{Y}_2, \vec{Y}_3$ the diffusion tensor has a form

$$\begin{pmatrix} \lambda_1 & 0 & 0 \\ 0 & \lambda_2 & 0 \\ 0 & 0 & \lambda_3 \end{pmatrix}$$

and the kick of the ion momentum along the \vec{Y}_i direction can be taken as $\sqrt{\lambda_i}$. In this case the kick of horizontal momentum component, for instance, can be expressed as follows:

$$P_x(t + \Delta t) = P_x(t) + \sqrt{\Delta t} \left(\frac{Y_{1,x}}{|Y_1|} \sqrt{\lambda_1} \xi_1 + \frac{Y_{2,x}}{|Y_2|} \sqrt{\lambda_2} \xi_2 + \frac{Y_{3,x}}{|Y_3|} \sqrt{\lambda_3} \xi_3 \right) , \quad (5.40)$$

and similar for y and z components. Correspondingly the coefficients $C_{i,j}$ can be written as:

$$C_{i,j} = \frac{Y_{j,i}}{|Y_j|} \sqrt{\lambda_j} . \quad (5.41)$$

The norm of the eigenvector is determined as usual

$$|Y| = \sqrt{Y_x^2 + Y_y^2 + Y_z^2} .$$

For IBS process (or for diffusion in an electron bunch), one can show analytically, that all the eigenvalues are positive numbers. In this case the described algorithm can be used for reduction of Fokker-Plank equation to Langevin one. The algorithm includes the following steps.

1. From the diffusion tensor components one needs to calculate eigenvalues in accordance with characteristic equation

$$\begin{vmatrix} D_{x,x} - \lambda & D_{x,y} & D_{x,z} \\ D_{x,y} & D_{y,y} - \lambda & D_{y,z} \\ D_{x,z} & D_{y,z} & D_{z,z} - \lambda \end{vmatrix} = 0$$

2. For each eigenvalue one needs to find corresponding eigenvector.
3. In accordance with (5.41) to calculate $C_{i,j}$
4. To realize the kick in accordance with (5.33).

This algorithm is under development now.

REFERENCES

1. I.N.Meshkov, A.O.Sidorin, A.V.Smirnov, E.M.Syresin, G.V.Trubnikov, P.R.Zenkevich, "Simulation of Electron Cooling Process in Storage Rings Using Betacool Program", proceedings of Beam Cooling and Related Topics, Bad Honnef, Germany, 2001.
2. I.N.Meshkov, R. Maier et al, "Electron cooling application for luminosity preservation in an experiment with internal targets at COSY", Dubna 2001, Jul-4031.
3. B.Autin, "Fast betatron cooling in antiproton accumulator", CERN/PS-AA/82-20
4. H.Stockhorst, Design deliberations for a stochastic cooling system at HESR, FZJ
5. T.Katayama and N.Tokuda, Part. Acc., 1987, Vol. 21
- 6.M.Babzien, I.Ben-zvi, I.Pavlishin, I.Pogorelsky, V.Yakimenko, A.Zholents, M.Zolotorev. Optical stochastic cooling for RHIC using optical parametric amplification. Phys.Rev. volume 7, PRST-AB (2004).
7. D.Möhl, CERN Accelerator School Report, CERN 87-03 (1987), p.453.